Discovery of a series of indazole TRPA1 antagonists

David C. Pryde[*,a,†] Brian E. Marron,[b] Christopher W. West,[b] Steven Reister,[b] George Amato,[b] Katrina Yoger,[b] Brett Antonio,[b] Karen Padilla,[b] Peter J. Cox,[c] Jamie Turner,[c] Joseph S. Warmus,[d] Nigel A. Swain,[a] Kiyoyuki Omoto[a], John H. Mahoney[b] and Aaron C. Gerlach[b]

[a]Pfizer Worldwide Medicinal Chemistry, Neuroscience and Pain Research Unit, Portway Building, Granta Park, Great Abington, Cambridgeshire, CB21 6GS, UK. [b]Pfizer Neuroscience and Pain Research Unit, 4222 Emperor Boulevard, Suite 350, Durham, North Carolina, NC27703, USA. [c]Pfizer Neuroscience and Pain Research Unit, Portway Building, Granta Park, Great Abington, Cambridgeshire, CB21 6GS, UK. [d]Pfizer Worldwide Medicinal Chemistry, Neuroscience and Pain Research Unit, Groton, CT, USA.

Supplementary Information

1. Compound Synthesis

General

All chemicals, reagents and solvents were purchased from commercial sources and used without further purification. All reactions were performed under an atmosphere of nitrogen unless otherwise noted.

NMR spectra were recorded on a Varian Unity 400 at room temperature at 400MHz. Chemical shifts are expressed as parts per million (δ) relative to residual solvent as an internal reference.

Characteristic chemical shifts (δ) are given using conventional abbreviations for designation of major peaks: e.g. s, singlet; d, doublet; t, triplet; q, quartet; m, multiplet; br, broad. The following abbreviations have been used for common solvents: $CDCl_3$, deuterochloroform; d6-DMSO, deuterodimethylsulphoxide; CD_3OD, deuteromethanol.

Mass spectra were recorded by direct flow analysis using positive and negative atmospheric pressure chemical ionization scan modes. A Waters APcI/MS model ZMD mass spectrometer equipped with a Gilson 215 liquid handling system was used to carry out the experiments. Mass spectrometry analysis was also obtained by reversed phase HPLC gradient method for chromatographic separation. Molecular weight identification was recorded by positive and negative electrospray ionization (ESI) scan modes. A Waters/Micromass ESI/MS model ZMD or LCZ mass spectrometer equipped with Gilson 215 liquid handling system and HP 1100 DAD was used to carry out the experiments. Purity determinations on test compounds were carried out either by elemental analysis or by LCMS analysis. All test compounds for which biochemical data is reported are of >95% purity.

Column chromatography was performed with Baker silica gel 40 μm; J.T. Baker, Phillipsburg, NJ) in glass columns under low nitrogen pressure. Where HPLC chromatography is referred to below, the column used was a Waters Sunfire C18 column, 50 x 4.6 mm using mixtures of formic acid in water (typically 0.1% formic acid in water) or acetonitrile (typically 0.1% formic acid in acetonitrile) as eluent at a flow rate of 1.5 mL/min, unless otherwise indicated. Compounds were detected by UV absorption (225 nm) and electrospray mass ionization.

Abbreviations

APCI; atmospheric pressure chemical ionisation mass spectrum

DCE; dichloroethane

DCM; dichloromethane

DIPEA; diisopropylethylamine

DMAP; dimethylaminopyridine

DMF; dimethyl formamide

DMSO; dimethyl sulfoxide

dppf; 1,1-bis(diphenylphosphino)ferrocene

ESI; electrospray ionization

EtOAc; ethyl acetate

EtOH; ethanol

HCl; hydrochloric acid

HPLC; high pressure liquid chromatography

IPA; isopropylamine

LCMS; liquid chromatography mass spectrum

LRMS; low resolution mass spectrum

$MgSO_4$; magnesium sulfate

m/z; mass spectrum peak, mass to charge ratio

$NaHCO_3$; sodium bicarbonate

NH_4Cl; ammonium chloride

$Na_2S_2O_3$; sodium thiosulfate

Na_2SO_4; sodium sulfate

NMR; nuclear magnetic resonance

PCl_5; phosphorus pentachloride

PMBCl; paramethoxybenzyl chloride

ppm; parts per million

Rt; retention time

UV; ultraviolet

Synthesis of Compound 10

N-(4-chlorophenyl)-6-(trifluoromethyl)-1*H*-indazol-3-amine

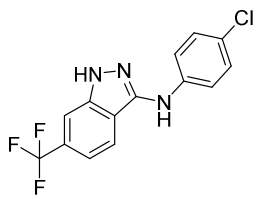

To a solution of *N*-(4-chlorophenyl)-2-fluoro-4-(trifluoromethyl)-thiobenzamide (250 mg, 0.75mmol) in EtOH (10 mL) was added hydrazine (1 mL, 31.9mmol). The mixture was heated at 50°C in a sealed tube for 16h, and then reduced in volume under reduced pressure. The residue was taken up in 10 mL MeCN and heated at 150°C in a microwave reactor for 1h. The reaction was concentrated *in vacuo*. Column chromatography using 30% EtOAc in hexanes provided the title compound as a white solid (230 mg, 94%). ^{1}H NMR ($CDCl_3$, 400MHz): δ 6.38 (m, 1H), 7.26-7.43 (m, 4H), 7.70 (s, 2H), 9.70 (s, 1H). HRMS: m/z found 312.0500 $[M+H]^+$. $C_{14}H_{10}ClF_3N_3$ requires m/z 312.0510. LCMS, formic acid in water/MeCN mobile phase: Rt 1.62 min, m/z 312 $[M+H]^+$, purity 100%.

Compounds, 8, 9, 11, 12 and 13 were all made analogously to compound 10.

N-(6-chloropyridin-3-yl)-6-(trifluoromethyl)-1*H*-indazol-3-amine (**8**), prepared from *N*-(6-chloropyridin-3-yl)-2-fluoro-4-(trifluoromethyl)-thiobenzamide and hydrazine. LCMS m/z 314 $[M+H]^+$, purity 98%.

6-(trifluoromethyl)-N-[6-(trifluoromethyl)pyridine-3-yl]-1H-indazol-3-amine (**9**), prepared from 2-fluoro-4-(trifluoromethyl)-*N*-[6- trifluoromethyl)pyridine-3-yl]-thiobenzamide and hydrazine. LCMS m/z 347 $[M+H]^+$, purity 98%.

N-(6-chloropyridin-3-yl)-1-methyl-6-(trifluoromethyl)-1*H*-indazol-3-amine (**11**), prepared from *N*-(6-chloropyridin-3-yl)-2-fluoro-4-(trifluoromethyl)-thiobenzamide and methyl hydrazine. LCMS m/z 328 $[M+H]^+$, purity 100%.

N-(6-chloropyridin-3-yl)-*N*-methyl-6-(trifluoromethyl)-1*H*-indazol-3-amine (**12**), prepared from *N*-(6-chloropyridin-3-yl)-2-fluoro-*N*-methyl-4-(trifluoromethyl)-thiobenzamide and methyl hydrazine. LCMS m/z 328 $[M+H]^+$, purity 100%.

N-(6-chloropyridin-3-yl)-*N*,1-dimethyl-6-(trifluoromethyl)-1*H*-indazol-3-amine (**13**), prepared from *N*-(6-chloropyridin-3-yl)-2-fluoro-*N*-methyl-4-(trifluoromethyl)-thiobenzamide and hydrazine. LCMS m/z 342 $[M+H]^+$, purity 100%.

Synthesis of Compound 14

N-(4-chlorophenyl)-1*H*-indazol-3-amine

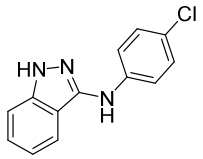

To a solution of *N*-(4-chlorophenyl)-2-fluorobenzamide (100 mg, 0.4mmol) in toluene (1.8 mL) and pyridine (0.2 mL) was added 2,4-bis-(4-methoxyphenyl)-2,4-dithioxo-1,2,3,4-dithia-diphosphetane (210 mg, 0.52mmol). The mixture was heated at reflux for 2h and then allowed to cool to room temperature. EtOAc (2 mL), saturated sodium bicarbonate solution (2 mL) and water (0.8 mL) were added. The mixture was stirred vigorously for 30 min and then the organic layer separated, dried over Na_2SO_4 and concentrated *in vacuo*. The resulting yellow solid was dissolved in EtOH (2 mL), treated with hydrazine (0.04 mL, 1.2mmol) and the mixture heated at reflux for 2h. The EtOH was removed and replaced with n-BuOH (2 mL) and the whole heated at 115°C for 15h. After this time, the reaction was allowed to cool to room temperature and EtOAc (4 mL), brine (2 mL) and water (0.8 mL) added. The organic layer was removed and filtered through a short pad of celite and then concentrated *in vacuo*. Column chromatography on silica gel using 40% EtOAc in hexanes as eluent to provide the title compound* as an off-white solid (5 mg, 5%). LRMS m/z: found 244 $[M+H]^+$. $C_{13}H_{11}N_3Cl$ requires m/z 244. ^{1}H NMR (400MHz, d6-DMSO): δ 7.16 (d, *J* = 8.6 Hz, 1H), 7.24-7.41 (m, 2H), 7.43-7.49 (m, 2H), 7.86-8.06 (m, 2H), 9.22 (s, 1H), 12.24 (s, 1H). LCMS, formic acid in water/MeCN mobile phase: Rt 2.46 min, m/z 244 $[M+H]^+$, purity 100%.

* Burmistrov, S. I. and Belykh, V. S., *Khimiya Geterotsiklicheskikh Soedinenii* , **1973**, 2, 249-51.

Synthesis of Compound 15

N-(3,4-difluorophenyl)-6-(trifluoromethyl)-1*H*-indazol-3-amine

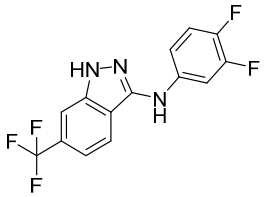

To a solution of N-(3,4-difluorophenyl)-2-fluoro-4-trifluoromethyl-benzamide (128 mg, 0.4mmol) in DCE (1.2 mL) was added PCl_5 (1.02 mg, 0.48mmol). The mixture was heated at reflux for 2h, and then

reduced in volume under reduced pressure and THF (8 mL) added. The mixture was cooled in an ice bath and hydrazine (0.19 mL, 6mmol) was added in one portion and the resulting mixture stirred at room temperature for 2h. The reaction was then concentrated *in vacuo* and the residue was partitioned between DCM and a 1:1 solution of saturated aqueous brine and 1M NaOH solution. After vigorous stirring, the organic layer was separated, dried over Na_2SO_4 and concentrated to provide an off-white solid. This solid was dissolved in 0.8 mL NMP and pyridine (0.4 mL, 0.48mmol) and heated at 80°C overnight. The reaction was partitioned between EtOAc and water, washed with saturated aqueous $NaHCO_3$ solution, brine and then the organic layer was separated, dried over Na_2SO_4 and concentrated *in vacuo*. Column chromatography using 30% EtOAc in hexanes provided the title compound as a white solid (96 mg, 76%). ^{1}H NMR (d6-DMSO, 400MHz): δ 7.35-7.43 (m, 3H), 7.80 (s, 1H), 7.90 (ddd, *J* 13.4, 7.0, 2.8 Hz, 1H), 8.19 (d, *J* = 13.6 Hz, 1H), 9.42 (s, 1H). HRMS: m/z found 314.0713 $[M+H]^+$. $C_{14}H_9F_5N_3$ requires m/z 314.0711. LCMS, formic acid in water/MeCN mobile phase: Rt 1.99 min, m/z 314 $[M+H]^+$, purity 100%.

Synthesis of Compound 16

6-chloro-*N*-(3,4-difluorophenyl)-1*H*-indazol-3-amine

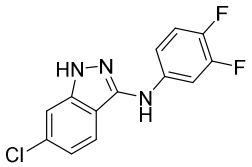

To a solution of 4-chloro-N-(3,4-difluorophenyl)-2-fluoro-benzamide (561 mg, 1.96mmol) in DCE (1.2 mL) was added PCl_5 (490 mg, 2.4mmol). The mixture was heated at reflux for 2h, and then reduced in volume under reduced pressure and THF (8 mL) added. The mixture was cooled in an ice bath and hydrazine (0.92 mL, 29mmol) was added in one portion and the resulting mixture stirred at room temperature for 1h. The reaction was then concentrated *in vacuo* and the residue was partitioned between DCM and a 1:1 solution of saturated aqueous brine and 1M NaOH solution. After vigorous stirring, the organic layer was separated, dried over Na_2SO_4 and concentrated to provide an off-white solid. This solid was dissolved in 4 mL NMP and pyridine (0.19 mL, 2.4mmol) and heated at 80°C overnight. The reaction was partitioned between EtOAc and water, washed with saturated aqueous $NaHCO_3$ solution, brine and then the organic layer was separated, dried over Na_2SO_4 and concentrated *in vacuo*. Column chromatography using 30% EtOAc in hexanes provided the title compound as a white solid (96 mg, 76%). ^{1}H NMR (d6-

DMSO, 400MHz): δ 7.35-7.43 (m, 3H), 7.80 (s, 1H), 7.90 (ddd, *J* 13.7, 7.0, 2.7 Hz, 1H), 8.19 (d, *J* 8.3 Hz, 1H), 9.42 (s, 1H). HRMS: m/z found 280.0449 $[M+H]^+$. $C_{13}H_9ClF_2N_3$ requires m/z 280.0448. LCMS, formic acid in water/MeCN mobile phase: Rt 1.89 min, m/z 280 $[M+H]^+$, purity 100%.

Synthesis of Compound 17

N-(3,4-difluorophenyl)-6-(trifluoromethoxy)-1*H*-indazol-3-amine

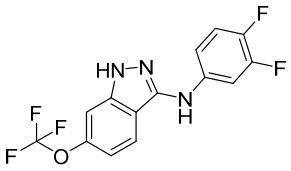

A solution of *N*-(3,4-difluorophenyl)-2-fluoro-4-(trifluoromethoxy)benzamide (167.6 mg, 0.50mmol) in 1 mL DCE was treated with PCl_5 (125 mg, 0.6mmol) and the reaction mixture was heated at reflux for 2h. It was then allowed to cool, was concentrated *in vacuo* and then dissolved in THF and added to a solution of hydrazine (235 µL, 7.50mmol) in 2 mL of dry THF. The reaction was stirred at room temperature for 1h and then concentrated *in vacuo*. The residue was partitioned between DCM and a 1:1 solution of saturated aqueous brine and 1M NaOH solution. The organic layer was separated, dried over Na_2SO_4 and concentrated to provide a light orange solid. This solid was dissolved in 4 mL NMP and pyridine (48.5 µL, 0.60mmol) and heated at 80°C overnight. The reaction was partitioned between EtOAc and water, washed with saturated aqueous $NaHCO_3$ solution, brine and then the organic layer was separated, dried over Na_2SO_4 and concentrated *in vacuo*. Column chromatography using 10% DCM in hexanes provided the title compound as a white solid (104 mg, 63%). ^{1}H NMR (MeOD, 400MHz): δ 6.97 (d, *J* 8.3 Hz, 1H), 7.14 (td, *J* = 10.4, 9.0 Hz, 1H), 7.21-7.34 (m, 2H), 7.72 (ddd, *J* 13.7, 7.0, 2.7 Hz, 1H), 7.91 (d, *J* 8.3 Hz, 1H). HRMS: m/z found 330.0657 $[M+H]^+$. $C_{14}H_9F_5N_3O$ requires m/z 330.0660. LCMS, formic acid in water/MeCN mobile phase: Rt 1.97 min, m/z 330 $[M+H]^+$, purity 100%.

Synthesis of Compound 18

N-(3,4-difluorophenyl)-6-(2-(trifluoromethoxy)phenyl)-1*H*-indazol-3-amine

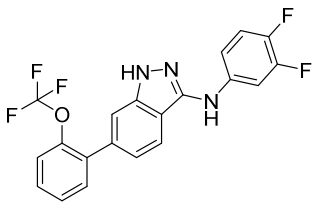

[1,1-bis(diphenylphosphino)ferrocene]dichloropalladium(II) (10.5 mg, 0.014mmol) was added to a suspension of 6-bromo-*N*-(3,4-difluorophenyl)-1*H*-indazol-3-amine (46.5 mg, 0.14mmol), 2-(trifluoromethoxy)benzeneboronic acid (35.4 mg, 0.17mmol) and sodium carbonate (45.6 mg, 0.43mmol) in IPA (3 mL) and water (1 mL). The reaction was heated in a microwave reactor at 150°C for 30min and then concentrated *in vacuo*. The residue was partitioned between EtOAc and water and the organic layer was then separated, washed with saturated brine and then dried over Na_2SO_4 and concentrated *in vacuo*. Column chromatography on silica gel using 10% DCM in hexanes as eluent to provide the title compound as a waxy solid (58 mg, 100%). ^{1}H NMR (400MHz, d6-DMSO): δ 7.16 (d, *J* 12.0 Hz, 1H), 7.24-7.41 (m, 2H), 7.43 (s, 1H), 7.43-7.49 (m, 2H), 7.54-7.64 (m, 1H), 7.87 (ddd, *J* 12.0, 7.5, 3.0Hz, 1H), 8.02 (d, *J* 12.0 Hz, 1H), 9.22 (s, 1H), 12.24 (s, 1H). HRMS: m/z found 406.0977 $[M+H]^+$. $C_{20}H_{13}F_5N_3O$ requires m/z 406.0973. LCMS, formic acid in water/MeCN mobile phase: Rt 1.57 min, m/z 406 $[M+H]^+$, purity 100%.

Compound 19 was made analogously to 18.

N,6-bis(3,4-difluorophenyl)-1*H*-indazol-3-amine (**19**), prepared from 6-bromo-*N*-(3,4-difluorophenyl)-1*H*-indazol-3-amine and 3,4-difluorobenzene boronic acid. LCMS, formic acid in water/MeCN mobile phase: Rt 1.43 min, m/z 358 $[M+H]^+$, purity 100%.

Synthesis of Compound 20

N-(3,4-difluorophenyl)-6-(trifluoromethyl)-1*H*-pyrazol[4,3-b]pyridine-3-amine

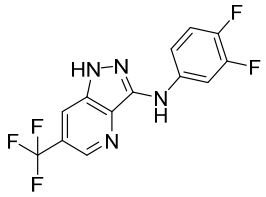

1-tert-butyl-6-(trifluoromethyl)-1H-pyrazol[4,3-b]pyridine-3-amine (700 mg, 3mmol) in 1,4-dioxane (15 mL) and potassium phosphate (860 mg, 4.1mmol) was treated with 1-bromo-3,4-difluorobenzene (620 µL, 5.2mmol) in a small pressure vial and purged with argon gas. 9,9-Dimethyl-4,5-bis(diphenylphosphino)xanthene (160 mg, 0.27mmol) and tris(dibenzylideneacetone)dipalladium(0) (120 mg, 0.14mmol) was added, the vial sealed and then heated at 110°C for 2 days. The mixture was cooled, diluted with water and extracted with EtOAc and then dried over Na_2SO_4 and concentrated *in*

vacuo. Column chromatography using 30% EtOAc in hexanes provided a white solid, which was taken up in formic acid (11 mL, 290mmol) and heated at 60°C for 4h and then at room temperature overnight. The mixture was concentrated *in vacuo*, diluted with EtOAc and saturated sodium bicarbonate and the organic layer separated, dried over Na_2SO_4 and concentrated *in vacuo*. The resulting oil was purified by HPLC to afford the title compound as a white solid (8 mg, 9%). LRMS: found m/z 315 $[M+H]^+$. $C_{13}H_8F_5N_4$ requires 315. ^1H NMR ($CDCl_3$, 400MHz): δ 7.07 (td, *J* = 10.4, 9.0 Hz, 1H), 7.24 (dddd, *J* = 8.6, 4.3, 2.6, 1.6 Hz, 1H), 7.65-7.81 (m, 2H), 9.12 (s, 1H). Found C, 49.46; H, 2.12; N, 17.86%. $C_{13}H_7F_5N_4$ requires C, 49.69; H, 2.25; N, 17.83%.

Synthesis of Compound 22

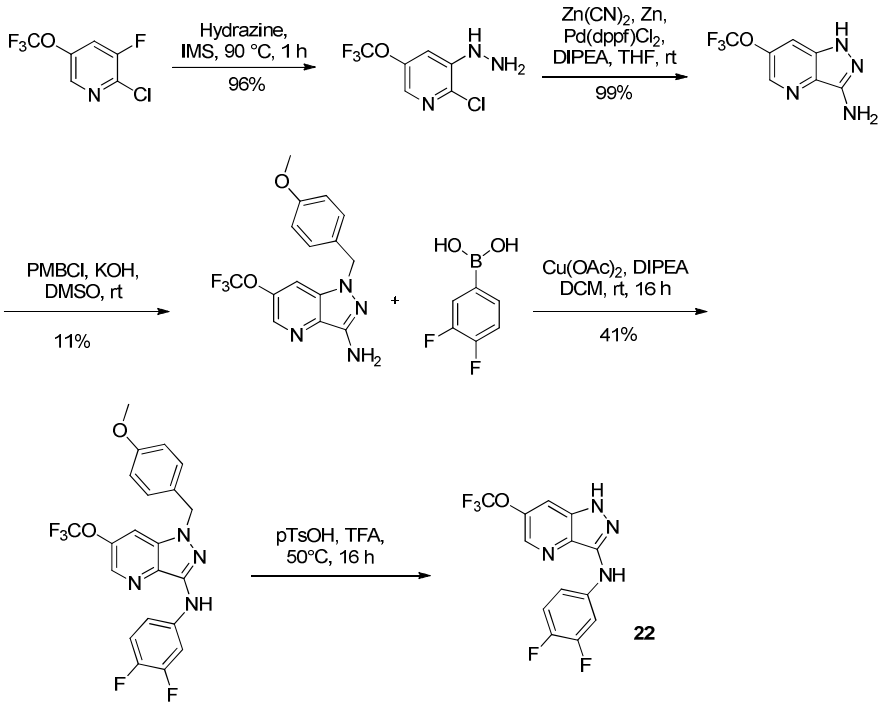

Step 1

2-chloro-3-hydrazinyl-5-(trifluoromethoxy)pyridine

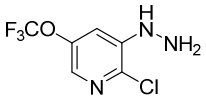

2-chloro-3-fluoro-5-trifluoromethoxypyridine (10 g, 46mmol) was dissolved in 25 mL ethanol. Hydrazine (15 mL) was then added and the mixture heated at 90°C for 30 min. The solvent was evaporated to

dryness and a mixture of water, EtOAc and saturated aqueous $NaHCO_3$ added. The organic layer was separated and dried over Na_2SO_4 and concentrated *in vacuo*. The solvent was then evaporated to give 10.56 g (~95% yield) of a yellow-green oil which was used without further purification.

Step 2

6-(trifluoromethoxy)-1*H*-pyrazolo[4,3-*b*]pyridine-3-amine

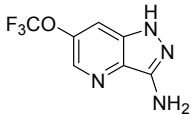

The hydrazide from Step 1 (10.06 g, 44mmol) was dissolved in 80 mL DMF. Argon was passed through the mixture for 10 min. Then zinc cyanide (13.9 g, 120mmol), Zn (0.56 g, 8.1mmol) and the catalyst bis(diphenylphosphino)ferrocene dichloropalladium (II) (2.8 g, 3.8mmol) added. The reaction mixture was heated at 120°C for 30 min. A mixture of water, EtOAc and saturated aqueous NH_4Cl was added and the mixture was filtered. The filtrate was separated and the organic layer dried over Na_2SO_4 and concentrated *in vacuo*. The residue was chromatographed using EtOAc in hexanes in a gradient of 0-100% to give 10 g (100% yield) of the product as a dark oil. LRMS: found m/z 219 $[M+H]^+$. $C_7H_5N_4OF_3$ requires 219.

Step 3

1-(4-methoxybenzyl)-6-(trifluoromethoxy)-1H-pyrazolo[4,3-b]pyridin-3-amine

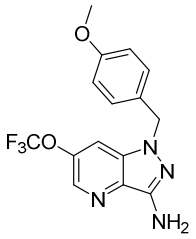

The amine (1g, 5mmol) was dissolved in DMSO (10 mL) and potassium hydroxide (493 mg, 8.8mmol) added. The mixture was stirred for 15 min at room temperature and then 4-methoxybenzylchloride (718 mg, 4.6mmol) added in one portion. The reaction was stirred at room temperature overnight. Saturated brine, water, EtOAc and saturated $NaHCO_3$ were all added. The organic layer was separated, dried over Na_2SO_4 and concentrated *in vacuo*. The residue was then chromatographed using a gradient of EtOAc in

hexanes of 0-100% to give the product as a yellow solid (640 mg, 40%). LRMS: m/z 339 $[M+H]^+$. $C_{15}H_{13}N_4O_2F_3$ requires 339.

Step 4

N-(3,4-difluorophenyl)-1-(4-methoxybenzyl)-6-(trifluoromethoxy)-1H-pyrazolo[4,3-b]pyridin-3-amine

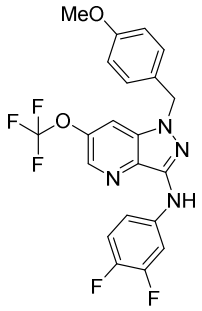

A suspension of copper (II) acetate (1.21 g, 6.65 mmol 1.5 eq) in DCM (45 mL) was stirred at room temperature for 5 minutes. After this time, 4A molecular sieves (3 g), 1-(4-methoxybenzyl)-6-(trifluoromethoxy)-1H-pyrazolo[4,3-b]pyridin-3-amine (1.50 g, 4.43 mmol, 1 eq), (3,4-difluorophenyl)boronic acid (2.10 g, 13.3 mmol, 3.0 eq) and diisopropylethylamine (1.16 mL, 6.65 mmol, 1.5 eq) were added and the reaction mixture was stirred in air (septum/needle) at room temperature for 16 hours. After this time further (3,4-difluorophenyl)boronic acid (2.10 g, 13.3 mmol, 3.0 eq), copper (II) acetate (1.21 g, 6.65 mmol 1.5 eq) and diisopropylethylamine (1.16 mL, 6.65 mmol, 1.5 eq) were added and allowed to stir at room temperature for 5 hours. After this time, the reaction mixture was filtered through arbocel and washed with DCM (50 mL), the filtrate was concentrated under reduced pressure to give the crude. The crude was purified by silica chromatography eluting from 20% to 80% DCM/heptane to give the title compound (875 mg, 44%) as a yellow solid. ^{1}H NMR ($CDCl_3$, 400MHz): δ 3.79 (s, 3H), 5.38 (s, 2H), 6.85-6.89 (m, 2H), 7.07-7.18 (m, 3H), 7.21-7.27 (m, 2H), 7.82 (ddd, *J* 12.0, 7.3, 2.8Hz, 1H), 8.28 (d, *J* 12.0 Hz, 1H). ^{19}F NMR ($CDCl_3$, 400MHz): δ -58 ppm (OCF_3), -136 ppm (ArF), -148 ppm (ArF). LCMS, formic acid in water/MeCN mobile phase: Rt 4.04 min, 451 $[M+H]^+$, purity 100%.

Step 5

N-(3,4-difluorophenyl)-6-(trifluoromethoxy)-1H-pyrazolo[4,3-b]pyridin-3-amine (**22**)

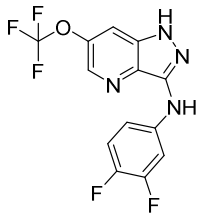

To a solution of N-(3,4-difluorophenyl)-1-(4-methoxybenzyl)-6-(trifluoromethoxy)-1H-pyrazolo[4,3-b]pyridin-3-amine (875 mg, 1.94 mmol, 1 eq) in trifluoroacetic acid (20 mL) was added p-toluenesulfonic acid monohydrate (1.11 g, 5.83 mmol, 3.0 eq). The reaction mixture was heated at 50 °C for 16 hours. After this time, the reaction was cooled to room temperature and trifluoroacetic acid was removed under reduced pressure. To the residue was added EtOAc (50 mL), H_2O (20 mL) and saturated $NaHCO_3$(aq) (50 mL). The phases were separated and the aqueous layer was further extracted with EtOAc (50 mL). The combined organic layers were washed with saturated $NaHCO_3$(aq) (100 mL), dried ($MgSO_4$), filtered and concentrated to give the crude. The crude was purified by silica chromatography eluting with 100% DCM to give the title compound with 9% starting material contaminated. It was further purified by trituation with 50% DCM/heptane (5 mL), the solid was collected by filtration and dried under reduced pressure to give the title compound (417 mg, 65%) as a white solid. ^{1}H NMR ($CDCl_3$, 400MHz): δ 7.10-7.32 (m, 2H), 7.60 (s, 1H), 7.82 (ddd, *J* 12.0, 7.5, 3.0Hz, 1H), 8.41 (s, 1H), 9.27 (s, 1H). ^{19}F NMR (CD_3OD, 400MHz): δ -60 ppm (OCF_3), -140 ppm (ArF), -152 ppm (ArF). LCMS, formic acid in water/MeCN mobile phase: Rt 3.18 min, 372.22 $[MH+MeCN]^+$, purity 98%. HRMS: m/z found 331.0609 $[M+H]^+$. $C_{13}H_8F_5N_4O$ requires m/z 331.0613. Found C, 47.33; H, 2.16; N, 16.76%. $C_{13}H_7F_5N_4O$ requires C, 47.29; H, 2.14; N, 16.97%.

Compounds 21 and 23 were made analogously to compound 22.

N-(3,4-difluorophenyl)-6-(trifluoromethyl)-1*H*-pyrazolo[4,3-*c*]pyridin-3-amine (**21**), prepared starting from 3-amino-6-bromo-1*H*-indazole. LCMS m/z 315 $[M+H]^+$, purity 100%.

N-(5-fluoropyridin-2-yl)-6-(trifluoromethoxy)-1*H*-pyrazolo[4,3-*b*]pyridine-3-amine (**23**), prepared starting from 2-chloro-3-fluoro-5-trifluoromethoxypyridine. LCMS m/z 314 $[M+H]^+$, purity 97%.

Synthesis of Compound 28

3-(4-cyanophenyl)-*N*-(2-methoxyethyl)-1*H*-indazole-6-carboxamide

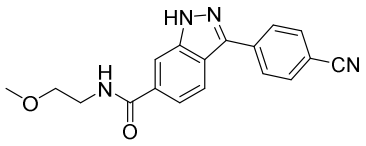

A mixture of 3-bromo-*N*-(2-methoxyethyl)-1*H*-indazole-6-carboxamide (93mg, 0.31 mmol), 4-cyanophenylboronic acid (138mg, 0.939 mmol), *bis*(di-*tert*-butyl(4-dimethylaminophenyl)phosphine)dichloropalladium(II) (6.3mg, 0.008mmol) and sodium carbonate (99mg, 0.94mmol) was taken up in a mixture of IPA (3 mL) and water (1.5 mL) and heated in a microwave reactor under Argon for 30 min at 120°C. Upon cooling to room temperature, the mixture was diluted with EtOAc and water and the organic layer was separated, washed with brine and then dried over Na_2SO_4 and concentrated *in vacuo*. The resulting yellow solid was purified by column chromatography using 5% MeOH in DCM as eluent to afford the product as a white solid (45 mg, 45%). LRMS: found m/z 319 [M-H]. $C_{18}H_{15}N_4O_2$ requires 319. ^{1}H NMR (400MHz, $CDCl_3$): δ 3.26 (s, 3H), 3.46-3.58 (m, 4H), 7.72 (d, *J* = 8.3Hz, 1H), 8.00 (d, *J* = 8.2Hz, 2H), 8.16-8.22 (m, 1H), 8.25 (d, *J* = 8.2Hz, 2H), 8.75 (m, 1H). Found C, 67.53; H, 5.02; N, 17.42%. $C_{18}H_{16}N_4O_2$ requires C, 67.49; H, 5.03; N, 17.49%.

Synthesis of Compound 33

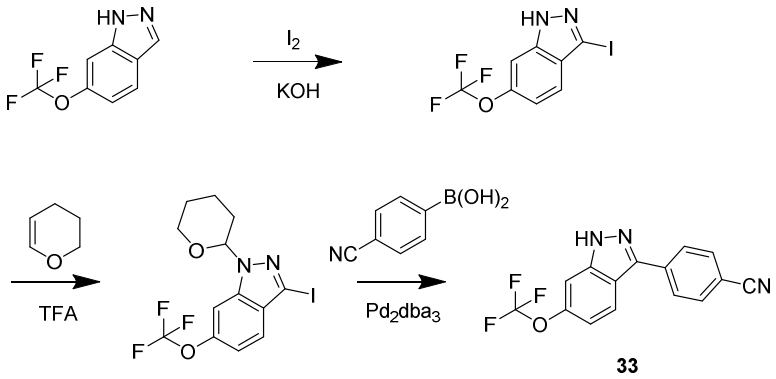

Step 1

3-iodo-6-(trifluoromethoxy)-1*H*-indazole

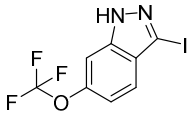

6-Trifluoromethoxy-indazole (10g, 49mmol) was dissolved in 300 mL DMF, then solid KOH (10g, 180mmol) added and the mixture stirred at room temperature for 15 min. Iodine (41g, 160mmol) was then added and the dark mixture left to stir at room temperature overnight. EtOAc and a 10% aqueous solution of $Na_2S_2O_3$ was added. Stirring was continued for 10 min and the organic layer then separated, dried over Na_2SO_4 and concentrated *in vacuo*. Column chromatography using a gradient of EtOAc in hexanes of between 0-100%, provided the product as a white solid (6g, 40%). LRMS: found m/z 329 $[M+H]^+$. $C_8H_5N_2OF_3I$ requires 329. ^{1}H NMR (400MHz, $CDCl_3$): δ 7.16-7.34 (m, 1H), 7.52-7.69 (m, 2H).

Step 2

3-iodo-1-(tetrahydro-2*H*-pyran-2-yl)-6-(trifluoromethoxy)-1*H*-indazole

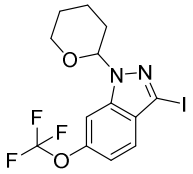

3-iodo-6-(trifluoromethoxy)-1H-indazole (2.72g, 8.3mmol) and trifluoroacetic acid (32 μL, 0.42mmol) in 50 mL of toluene was heated to 80°C. Dihydropyran (833 μL, 9.1mmol) was added slowly and the whole then heated at reflux overnight. The mixture was cooled to room temperature and then concentrated *in vacuo*. The resulting yellow oil was dissolved in a mixture of water and EtOAc and the organic layer was separated, washed with brine, then dried over Na_2SO_4 and concentrated *in vacuo*. Chromatography on silica with 10% EtOAc in hexanes as eluant provided the protected indazole as a viscous yellow gum (2.51g, 73%). LRMS: found m/z 413 $[M+H]^+$. $C_{13}H_{13}N_2O_2F_3I$ requires 413. ^{1}H NMR (400MHz, $CDCl_3$): δ 1.62-1.86 (m, 3H), 2.03-2.23 (m, 2H), 2.50-2.62 (m, 1H), 3.73-3.82 (m, 1H), 4.01-4.08 (m, 1H), 5.71 (m, 1H), 7.17 (d, *J* = 8.2 Hz, 1H),7.46 (s, *J* = 8.2 Hz, 1H), 7.53 (d, 1H).

Step 3

4-(6-(trifluoromethoxy)-1*H*-indazol-3-yl)benzonitrile (**33**)

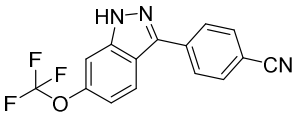

A mixture of 3-iodo-6-(trifluoromethoxy)-1H-indazole (3g, 9mmol), 4-cyanophenylboronic acid (2.04g, 13.7mmol) and sodium carbonate (1.98g, 18.3mmol) was taken up in 42 mL of a 3:1 mixture of IPA and

water and stirred at room temperature for 30 min. 341mg (0.48mmol) of bis(di-tert-butyl(4-dimethylaminophenyl)phosphine)dichloropalladium(II) was then added to the mixture stirring continued for a further 15 min. The yellow suspension was left stirring at 88°C for 5 hours and then cooled to room temperature, concentrated *in vacuo* and partitioned between EtOAc and a saturated aqueous solution of $NaHCO_3$. The organic phase was separated, washed with brine and then dried over Na_2SO_4 and concentrated *in vacuo*. The resulting light yellow solid was recrystallised from 15% DCM/hexanes to afford the product as an off white solid (1450 mg, 50%). LRMS: found m/z 304 $[M+H]^+$. $C_{15}H_9F_3N_3O$ requires 304. ^{1}H NMR (400MHz, MeOD): δ 7.16 (d, *J* = 7.1 Hz, 1H), 7.51 (t, *J* = 7.7 Hz, 1H), 7.62 (d, *J* = 8.2 Hz, 1H), 7.82-7.91 (m, 2H), 7.94-8.05 (m, 2H). HRMS: m/z found 304.0684 $[M+H]^+$. $C_{15}H_9F_3N_3O$ requires m/z 304.0692. Found C, 59.26; H, 3.02; N, 13.76%. $C_{15}H_8F_3N_3O$ requires C, 59.41; H, 2.66; N, 13.86%.

Synthesis of Compound 31

5-((6-(trifluoromethoxy)-1*H*-indazol-3-yl)amino)thiophene-2-carbonitrile

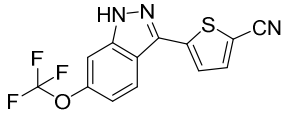

Following the above procedure, but using 3-iodo-6-(trifluoromethoxy)-1*H*-indazole and 5-cyanothiophen-2-ylboronic acid, the title compound was made in 58% yield.

^{1}H NMR (400MHz, MeOD): δ 7.18-7.30 (m, 1H), 7.48-7.56 (m, 1H), 7.79 (d, *J* = 4.3 Hz, 1H), 7.83 (d, *J* = 3.9 Hz, 1H), 8.17 (d, *J* = 8.6 Hz, 1H). LCMS, formic acid in water/MeCN mobile phase: Rt 1.60 min, m/z 310 $[M+H]^+$, purity 100%.

Synthesis of Compound 32

5-((6-(trifluoromethoxy)-1*H*-indazol-3-yl)amino)picolinonitrile

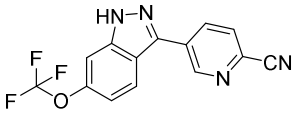

Following the above procedure, but using 3-iodo-6-(trifluoromethoxy)-1*H*-indazole and 2-cyanopyridyl-5-boronic acid ester, the title compound was made in 60% yield.

^{1}H NMR (400MHz, MeOD): δ 7.03-7.25 (m, 1H), 7.44 (s, 1H), 7.91 (d, *J* = 8.2 Hz, 1H), 8.10 (d, *J* = 8.6 Hz, 1H), 8.49 (dd, *J* = 8.2, 2.3 Hz, 1H), 9.27 (s, 1H). HRMS m/z: found 305.0643 $[M+H]^+$. $C_{14}H_8F_3N_4O$ requires

m/z 305.0645. LCMS, formic acid in water/MeCN mobile phase: Rt 1.47 min, m/z 305 $[M+H]^+$, purity 100%.

Compounds 24, 25, 26, 27, 29 and 30 were all made analogously to compound 33.

3-(3,4-difluorophenyl)-6-(trifluoromethyl)-1*H*-indazole (**24**) was made starting from 3-iodo-6-(trifluoromethyl)-1*H*-indazole and 3,4-difluorophenyl boronic acid. LCMS m/z $[M+H]^+$ 299, purity 99%.

3-(3,4-difluorophenyl)-6-(trifluoromethyl)-1*H*-pyrazolo[4,3-*b*]pyridine (**25**) was made starting from 3-iodo-6-(trifluoromethyl)-1*H*-pyrazolo[4,3-*b*]pyridine and 3,4-difluorophenyl boronic acid. LCMS m/z $[M+H]^+$ 300, purity 100%.

3-(4-fluorophenyl)-6-(trifluoromethoxy)-1*H*-pyrazolo[4,3-*b*]pyridine (**26**) was made starting from 3-iodo-6-(trifluoromethoxy)-1*H*-pyrazolo[4,3-*b*]pyridine and 4-fluorophenyl boronic acid. LCMS m/z $[M+H]^+$ 298, purity 98%.

N-[1-(cyclopropylmethyl)piperidin-4-yl]-3-(4-fluorophenyl)-1H-pyrazolo[4,3-*b*]pyridin-6-amine (**27**) was made starting from 3-iodo-6-nitro-1*H*-pyrazolo[4,3-*b*]pyridine and 4-fluorophenyl boronic acid. LCMS m/z $[M+H]^+$ 366, purity 99%.

3-(5-fluoro-1*H*-indol-2-yl)-6-(trifluoromethoxy)-1*H*-indazole (**29**) was made starting from 3-iodo-6-(trifluoromethoxy)-1*H*-indazole and 5-fluoro-1*H*-indol-2-yl-boronic acid. LCMS m/z $[M+H]^+$ 336, purity 100%.

3-(5-fluoro-1*H*-indol-2-yl)-6-(trifluoromethoxy)-1*H*-pyrazolo-[4,3-*b*]pyridine (**30**) was made starting from 3-iodo-6-(trifluoromethoxy)-1*H*-pyrazolo[4,3-*b*]pyridine and 5-fluoro-1*H*-indol-2-yl-boronic acid. LCMS m/z $[M+H]^+$ 337, purity 100%.

Synthesis of Compound 34

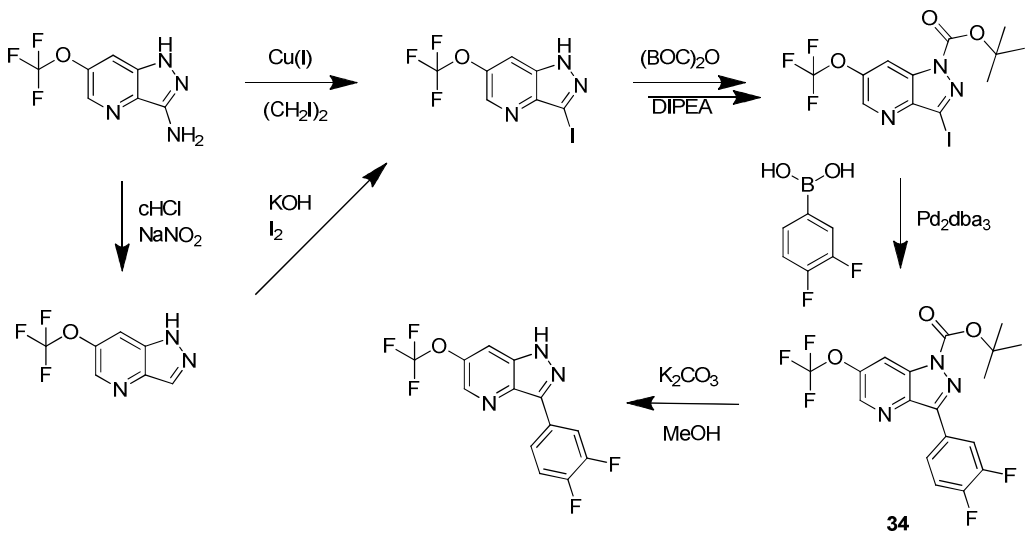

Step 1

3-iodo-6-(trifluoromethoxy)-1*H*-pyrazolo[4,3-*b*]pyridine

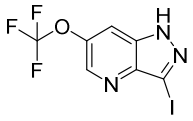

To a mixture of 6-(trifluoromethoxy)-1H-pyrazolo[4,3-b]pyridin-3-amine (1.0 g, 4.6mmol) in THF (10 mL) was added diiodomethane (1.8 mL, 23mmol). The mixture was cooled in an ice bath and to it was added copper(I) iodide (0.96 g, 5.0mmol) to give a yellow suspension. After 5 mins, amyl nitrite (1.8 ml, 14mmol) was added slowly. The mixture was stirred in an ice bath for 30 mins, the ice bath was removed and the mixture then stirred at room temperature for 1 hour. The mixture was heated at reflux for 1 hour and then allowed to cool to room temperature. EtOAc and 1N HCl were added. The organic layer was separated, dried over Na_2SO_4 and purified by column chromatography using EtOAc in hexanes, first at 10%, then increased to 30%. The product was obtained as a pale yellow solid (0.32 g, 21%). LRMS: found m/z 330 $[M+H]^+$. $C_7H_3F_3N_3IO$ requires 330.

Alternate route

6-(trifluoromethoxy)-1H-pyrazolo[4,3-b]pyridine

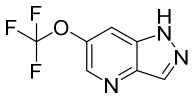

To a cool (0°C) solution of 6-(trifluoromethoxy)-1H-pyrazolo[4,3-b]pyridin-3-amine (1.3 g, 5.96 mmol, 1 eq) in H_2O (10 mL), acetic acid (15 mL) and concentrated HCl (5 mL) was added sodium nitrite (822 mg, 12 mmol, 2 eq) in solution in water (5 mL) then the mixture was stirred for 30 min at the same temperature, before the dropwise addition of hypophosphorous acid (50% solution in water, 15 mL, 92 mmol, 15 eq), the reaction was stirred at 0°C for 30 minutes then at room temperature for 2 hours. The reaction was then basified by a dropwise addition of 4M NaOH at 0°C, and partitioned with ethyl acetate (3 x 150 mL), the organic phase was washed with brine (150 mL), dried over magnesium sulfate, filtered and evaporated to give a brown residue (1 g, 4.92 mmol, 83%) that was used in the next step without further purification. LCMS, formic acid in water/MeCN mobile phase: Rt 2.07 min, 202 [M-H], purity 47%.

Alternate route

3-iodo-6-(trifluoromethoxy)-1H-pyrazolo[4,3-b]pyridine

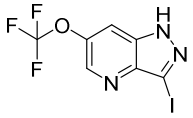

To a cool (0°C) solution of 6-(trifluoromethoxy)-1H-pyrazolo[4,3-b]pyridine (1 g, 4.92 mmol, 1 eq) in DMF (15 mL) was added potassium hydroxide (966 mg, 17 mmol, 3.5 eq) and iodine (2.5 g, 9.85 mmol, 2 eq) the mixture was stirred for 30 min at 0°C and 1 hour at room temperature, the mixture was then cooled to 0°C and quenched with 100 mL of saturated Na_2SO_3, the mixture was extracted with EtOAc (3 x 100 mL), the organic phase washed with brine (100 mL), dried over magnesium sulfate, filtered and evaporated. The residue was purified by column chromatography on silica gel (EtOAc/Heptane gradient 0 to 60%) to give a white solid (600 mg, 1.82 mmol, 37%). LCMS, formic acid in water/MeCN mobile phase: Rt 2.97 min, 330 $[M+H]^+$, purity 90%. ^{1}H NMR (DMSO d6, 400MHz): δ 8.20 (br s, 1 H), 8.61 (s, 1H), 13.99 (br s, 1H). ^{19}F NMR (DMSO d6, 400MHz): δ -57.3.

Step 2

tert-Butyl 3-iodo-6-(trifluoromethoxy)-1H-pyrazolo[4,3-b]pyridine-1-carboxylate

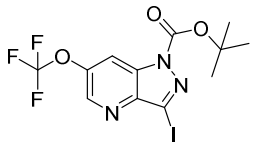

To a solution of 3-iodo-6-(trifluoromethoxy)-1H-pyrazolo[4,3-b]pyridine (548 mg, 1.67 mmol, 1 eq) DIPEA (0.58 mL, 3.33 mmol, 2 eq) and THF (10 mL) was added di-*tert*-butyl dicarbonate (400 mg, 1.83 mmol, 1.1 eq) and DMAP (20 mg, 0.17 mmol, 0.1 eq). The mixture was stirred for 3 hours. The reaction was then partitioned between 10% citric acid (100 mL) and EtOAc (2X100 mL). The organic layer was washed with brine (100 mL), dried over sodium sulfate, and concentrated to give the title compound as a white solid (900 mg, 2.1 mmol, 126%). ^{1}H NMR ($CDCl_3$, 400 MHz): δ 1.72 (s, 9 H), 8.34 (br s, 1 H), 8.64 (d, 1 H, *J*=2.2 Hz). LCMS, ammonium formate in water/MeCN mobile phase: Rt 1.88 min, 430 [M-H], purity 100%.

Step 3

tert-Butyl 3-(3,4-difluorophenyl)-6-(trifluoromethoxy)-1H-pyrazolo[4,3-b]pyridine-1-carboxylate

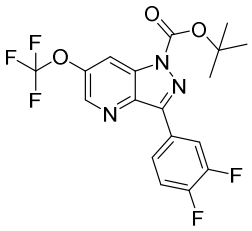

A solution of *tert*-butyl 3-iodo-6-(trifluoromethoxy)-1H-pyrazolo[4,3-b]pyridine-1-carboxylate (664 mg, 1.55 mmol, 1 eq), (3,4-difluorophenyl)boronic acid (318 mg, 2.01 mmol, 1.3 eq), Pd(dppf)Cl_2 (126 mg, 0.15 mmol, 0.1 eq) and cesium carbonate (1.01 g, 3.09 mmol, 2 eq) in dioxane (15 mL) was heated at 85°C in the microwave for 3 hours. The reaction was complete after this time. The mixture was filtered through a silica pad washed with EtOAc, the solvent was evaporated and the residue (1.2 g) took to the next step without further purification.

Step 4

Synthesis of 3-(3,4-difluorophenyl)-6-(trifluoromethoxy)-1H-pyrazolo[4,3-b]pyridine (**34**)

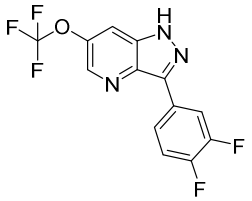

A solution of *tert*-butyl-3-(3,4-difluorophenyl)-6-(trifluoromethoxy)-1H-pyrazolo[4,3-b]pyridine-1-carboxylate (690 mg, 1.66 mmol, 1 eq) in THF (4 mL), MeOH (4 mL) and 4M potassium carbonate (4 mL) was heated to reflux for 2 hours, the mixture was cooled to room temperature and the solvent was

evaporated, and the residue was dry loaded on silica and purified by column chromatography on silica (EtOAc in heptane 10%) to give a white solid (400 mg, 1.27 mmol, 76%) the LCMS was 96% pure. The crude NMR spectrum showed some impurities, so the product was dissolved in 1 mL of TBME then heptane was slowly added until a precipitate started to form, the solid was filtered to give a white solid (304 mg, 0.96 mmol, 58%). LCMS, formic acid in water/MeCN mobile phase: Rt 1.47 min, 314 [M-H], purity 99%. ^{1}H NMR (MeOD, 400MHz): δ 7.35-7.42 (m, 1H), 7.96 (s, 1H), 8.30-8.34 (m, 1H), 8.39-8.44 (m, 1H), 8.60 (s, 1H). ^{19}F NMR (MeOD, 400MHz): δ -140.57, -140-90, -59.96. HRMS: m/z found 316.0506 $[M+H]^{+}$. $C_{13}H_7F_5N_3O$ calculated m/z 316.0504. Found C, 49.62; H, 1.95; N, 13.23%. $C_{13}H_6F_5N_3O$ requires C, 49.54; H, 1.92; N, 13.33%.

2. Plasmids and cell lines

Full-length human TRPA1 (hTRPA1) cDNA (Genbank accession Y10601) was cloned into inducible vector pcDNA5/TO (Invitrogen, Carlsbad, CA). DNA representing full-length opossum TRPA1 (oTRPA1, Monodelphis domestica XP001378427) was codon-optimized, synthesized and cloned into pcDNA5/TO. The hS5 chimera was generated by gene synthesis of human S5 DNA which was cloned (using seamless cloning technology) into opossum TRPA1 to replace oS5. The oS5 chimera was generated by synthesis of opossum S5 DNA which was cloned into human TRPA1 to replace hS5. This resulted in a 27 amino acid swap such that for the hS5 chimera, hTRPA1 amino acids 867-893 replaced oTRPA1 amino acids 870-896. For the oS5 chimera, oTRPA1 amino acids 870-896 replaced hTRPA1 amino acids 867-983. All gene synthesis and seamless cloning was performed by GenScript USA. Stable clonal cell lines for each chimeric construct were generated by transfecting chimera plasmid DNA into 293-T-REx cell line (Invitrogen) and selecting with 150ug/ml hygromycin and 5ug/ml blasticidin (at 37˚C with 10% CO_2). 1 ug/ml tetracycline was used to induce hTRPA1 expression for functional assays.

3. Whole-cell patch clamp electrophysiology

Whole-cell manual patch clamp recordings were obtained using patch pipettes with resistances of 1.5 to 3.0 MΩ when filled with the internal solution, consisting of (in mM) 90 CsCl, 32 CsF, 10 HEPES, 10 EGTA, 10 Cs_4 BAPTA, 1 $MgCl_2$, 5 Mg ATP, and 0.1 Na GTP, pH adjusted to 7.3 with CsOH. The external solution consisted of (in mM) 132 NaCl, 5.4 KCl, 1.8 $CaCl_2$, 0.8 $MgCl_2$, 10 HEPES, and 5 Glucose, pH adjusted to 7.4 with NaOH. To ensure complete dialysis with pipette solution, recordings began 1 min after establishment of whole-cell configuration. Subsequently, 150 µM cinnamaldehyde was perfused with the external solution to activate TRPA1 channels. Currents were recorded at room temperature with an Axopatch 200B amplifier and filtered at 1 kHz with a low-pass Bessel filter. Voltage protocols were elicited using Clampex 10.2 software and consisted of 150 msec. depolarizing ramps from -40 mV followed by 100 msec steps to +40 mV and then to -40 mV repeated every 5 seconds from a holding potential of 15 mV. Currents were digitized using a Digidata 1440A data acquisition interface and analyzed using Clampfit 10.2 software. For these experiments the average steady state current at -40 mV was analyzed for each test condition. For potency experiments, cumulative concentration-responses were generated. Individual concentration-response relationships were fitted to a logistic equation with floating potency, slope and Emax. Individual concentration-relationships were then normalized to their fitted Emax to visualize all data on a single graph. PatchXpress automated EP voltage protocol was same as manual patch and used custom scripting to determine steady-state block. For these experiments the internal solution was composed of (in mM) 60 CsCl, 30 CsF, 10 HEPES, 20 EGTA, 20 Cs_4 BAPTA, 1 $MgCl_2$, 5 Mg ATP, and 0.1 Na GTP, pH adjusted to 7.3 with CsOH. TRPA1 channels were activated with 300 µM cinnamaldehyde.

Data summary

Supplementary Table 1. Summary of biological data, replicates and standard deviations

All data is against the human channel unless otherwise stated

Compound no.	TRPA1 IC50 n numbers, SD FLIPR	TRPA1 mean IC50 (nM) FLIPR	TRPA1 est. IC50 n numbers, SD PXpress	TRPA1 est. IC50 (nM) PXpress	Rat TRPA1 est. IC50 n numbers, SD PXpress	Rat TRPA1 est. IC50 (nM) PXpress
8	-	-	N=4, SD 149	546	-	-
9	-		N=2	>10,000	-	-
10	N=2, SD 2202	3255	N=3, SD 8	42	N=10, SD 5	9
11	-	-	N=3	>10,000	-	-
13	-	-	N=2	>10,000	-	-
12	-	-	N=3	>10,000	-	-
14	-	-	N=2, SD 2586	11,700	-	-
20	-	-	N=2, SD 16	38	N=2, SD 4	23
15	N=2	>10,000	N=3, SD 28	53	N=2, SD 1	9
16	-	-	N=2, SD 18	111	N=7, SD 15	49
21	N=2, SD 602	3740	N=3, SD 102	645	-	-
17	-	-	N=3, SD 32	131	N=2	<100nM 96% @ 1μM
23	-	-	N=2, SD 1141	2537	N=4, SD 344	813
22	N=10, SD 159	332	N=2, SD 4	20	N=25, SD 5	11
18	-	-	N=2, SD 1623	1203	N=2	<100nM 99% @ 1μM
19	-	-	N=3, SD 240	3700	-	-
28	-	-	N=2, SD 784	2667	N=2, SD 112	453
33	N=5	>10,000	N=6, SD 140	686	N=30, SD 82	246
31	-	-	N=3, SD 19	74	N=8, SD	80

					64	
32	-	-	N=2, SD 209	1182	N=6, SD 41	271
25	-	-	N=3, SD 142	450	N=6, SD 99	255
24	-	-	N=6, SD 40	2100	N=4, SD 136	329
26	-	-	N=4, SD 8	257	N=2, SD 109	216
27	-	-	N=3, SD 1302	4630	N=4, SD 1189	1851
29	-	-	N=3, SD 384	748	N=2, SD 61	116
30	-	-	N=3, SD 7	91	N=6, SD 1	8
34	-	-	N=3, SD 9	134	N=2, SD 68	128

4. Binding site elucidation using protein chimeras

In order to establish the binding site of compounds such as 22 and 33, TRPA1 species ortholog chimeras were generated to identify the critical regions of interaction. Opossum TRPA1 (oTRPA1) was selected as the human (hTRPA1) chimeric partner because of divergence in the channel pore region (68% identity in S5-S6). Chimeric constructs were stably expressed in hEK293 cells and evaluated using manual whole-cell voltage clamp electrophysiology as has been described previously in *MedChemComm*, 2016, *7*, 2145-2158.

The figure below shows the potency of 22 against these species orthologs and chimeras. 22 was >1000X more potent against hTRPA1 (IC_{50}=20 nM) compared to oTRPA1 (IC_{50}>30microM). Because of this potency difference, hTRPA1/oTRPA1 chimeric constructs were designed to help elucidate the compound binding site (data not shown). A 27 amino acid sequence within the S5 helix was swapped and 22 potency tested. The potency of the compound positively correlated with the species source of this 27 amino acid S5 region. Gain of potency was observed when the S5 region of human TRPA1 was swapped into oTRPA1 (hS5, IC_{50}=132 nM). Loss of function was observed in the counterpart chimera (oS5, IC_{50}=16 microM). Taken together, these data suggest the activity of 22 at TRPA1 is dependent on the S5 helix.

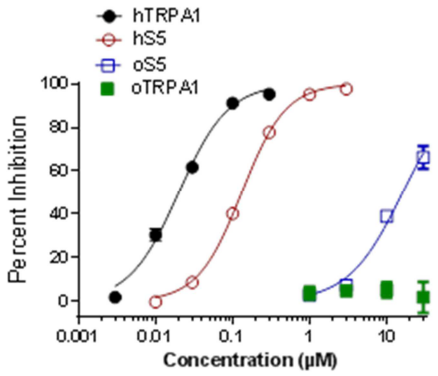

Supplementary Figure 1. Indazole potency is dependent on the TRPA1 S5 helix[1]

[1] hTRPA1/oTRPA1 chimeras were generated by swapping the 27 amino acid comprising S5. hS5 designates chimeras in which hTRPA1 amino acids 867-893 were swapped into oTRPA1. oS5 designates chimeras in which oTRPA1 amino acids 870-896 were swapped into hTRPA1. The mean IC50 (95% confidence interval, *n*) was (●) hTRPA1=0.020 µM (95% CI= 0.018-0.023 µM, *n*=6), (○)

hS5=0.132 µM (95% CI=0.126-0.138 µM , *n*=3), (□) oS5=16.1 µM (95% CI-13.5-19.3 µM, *n*=3) and (■) oTRPA1 = >30 µM (*n*=3).

5. Compound 33 selectivity

Ion channels

Supplementary Table 2. Ion channel selectivity data for 33

	IC_{50} (μM)	**Selectivity (fold)**
TRPA1 (human)	0.64 (MP 0.195)	
TRPA1 (rat)	0.20 (MP 0.195)	
Cardiac		
Kv7.1	1.4 (MP >3)	2.2 (MP >15)
hERG	>30	>46
Nav1.5	17.3	26.9
TRP		
TRPV1	27.0	41.9
TRPV3	>30 (MP >50)	>46 (MP >100)
TRPM8	>30 (MP >50)	>46 (MP >100)
Other		
Nav1.8	31.4 (MP >50)	48.8 (MP >100)
Nav1.1	14.5	22.5
Nav1.2	26.1	40.5
Nav1.6	28.7	44.5
Nav1.7	17.7	27.5
Cav2.2	29.9 (MP >50)	46.4 (MP >100)
Kv7.2/7.3	>30	>46

All data are the mean of at least two separate experiments, and were produced in a PX platform unless otherwise stated.

Broad ligand profiling

>10 μM on all receptors and transporters in a CEREP panel of 72 targets, except adenosine 2A (IC_{50} = 2 μM) and NE transporter (IC_{50} = 8 μM).

6. **Computational docking studies**

Having established using protein chimeras that compounds from the series relied on contacts within S5 for hTRPA1 activity, we sought to provide more granularity of critical residues of interaction using computational docking. Specific residues in the S5 region have been suggested to be involved in interactions with small molecule TRPA1 modulators. Xiao et.al found that agonist activity of menthol was ablated when the S5 domain is replaced with that of *Drosophila melanogaster* (*J Neurosci*, **2008**, *28*(39), 9640-9651). Sequence alignment suggested that Ser873 and Thr874 in the human protein were important (*J Mol Neurosci*, **2013**, *51*(3), 754-762) for small molecule binding. We docked exemplar compounds into the cryo-EM structure of human TRPA1 described by Paulsen et. al. (*Nature*, **2015**, *520*, 511-517) using compounds 22 and 33 and focused on a binding site in the region around Ser873 and Thr874.

As the human TRPA1 structure is a homo-tetramer, there are four equivalent binding sites. One binding site between chain A and B was selected for the docking calculations. Initial docking calculations, using the cryo-EM structure itself, were not successful. The calculations did not provide unique interaction modes of the compounds, likely because the reported cryo-EM structure was in complex with a ligand and a conformational change in the binding site was induced to accommodate the molecule. We created an ensemble of 500 human TRPA1 structure models in which the binding site conformation was randomized to introduce a degree of flexibility. The positions and dihedral angles of key residues such as Ser873, Thr874, and Phe909 could cover most viable conformations using this approach. Then, ligand binding poses were analysed through application of an ensemble docking program (created in-house) to the 500 human TRPA1 structure models. The compounds were docked to each of the 500 structures. Here, one docking process of a protein/ligand pair was set to provide 100 docking poses. This resulted in 50000 docking poses in total. The top 50 poses were selected based on docking score and evaluated for RMSD consistency. Interestingly, for both compounds 22 and 33, more than half of the 50 structures showed a unique binding mode with an RMSD consistency < 1.0 Å.

Supplementary Figure 2 shows an exemplar binding mode of compound 33. It appears that two hydrogen bond interactions stabilize the complex, formed between the OH group of Thr945 and the NH of the indole core, and the other being created between the CN group of the core and the OH group of Ser873. Thr874 lies close to the indazole 4-position and which could explain the quite specific SAR of the aromatic ring in this location. Introduction of an aromatic N at the 4-position (transformation from compound 24 to compound 25 and 29 to 30) resulted in enhancement of human TRPA1 potency,

potentially through the OH group of Thr874 forming a hydrogen bond to this N. A sub-pocket around Ser873 was not fully occupied, suggesting larger groups could be accommodated. The OCF_3 group on the 6-position of the indazole was located at the entrance of the binding site and directed toward bulk solvent (lipid membrane), suggesting that potency was less sensitive to modifications of substituents at this position. This assumption was consistent with compounds such as 28 with a much extended 6-substituent. This entrance region also attracted our attention from a species selectivity viewpoint. 27, whose 6-position contained a bulky amine substituent was more potent at rat than human protein. We propose that Val942 in human TRPA1 when mutated to Ile945 in rat TRPA1 supports a stronger hydrophobic interaction to these extended 6-substituents.

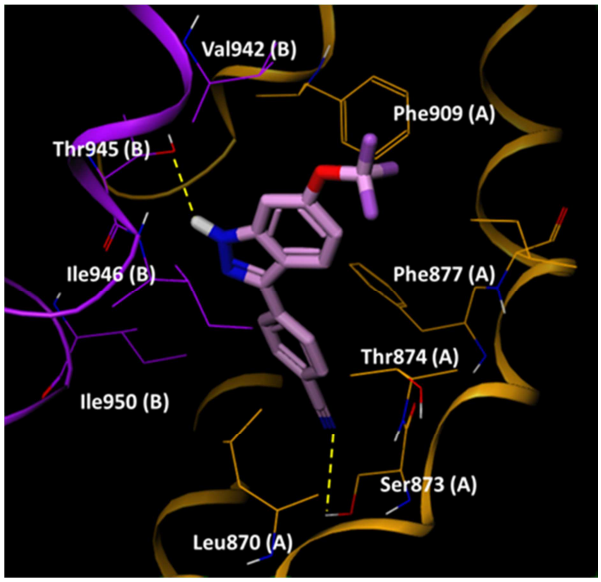

Supplementary Figure 2. 33 docked into the reported cryo-EM structure of TRPA1

A potential binding mode of compound 22 is shown in the two figures below. Two diagrams were created for visual clarity. There are two hydrogen bond interactions which stabilize ligand binding to the protein. The NH of the *1H*-pyrazolo[4,3-*b*]pyridine core formed a hydrogen bond interaction with the backbone carbonyl oxygen atom of Val942, which was unsatisfied in the apo structure due to the helix kink of S6. The NH linker between the two aromatic rings created a hydrogen bond interaction with the hydroxyl group of Thr874. These hydrogen bond interactions are consistent with the SAR of compounds 8, 11, and 13. Compound 8 showed an IC_{50} of 546 nM while both 11 and 13 are very weak ligands. The NH of the indazole and the linker NH of compound 8 was replaced by NMe in compound 11 and compound 13, respectively, and abrogation of activity of these compounds could be attributed to the

loss of the hydrogen bond interaction. Phe909, which was suggested to play a key role in the interaction with A967079 in the cryo-EM human TRPA1 structure, was engaged in a π–π stacking interaction with the *1H*-pyrazolo[4,3-*b*]pyridine ring. This interaction is further stabilized by a CH-π stacking interaction with the methyl group of Thr874, Ile878, and Leu881. Another π–π stacking interaction was seen between the 3,4-difluorophenyl ring and Phe877. A CH-π interaction with Leu956 on the other side of the ring system bolstered this interaction. The two fluorines projected into a hydrophobic environment created by Leu952, Met953, and Met912. This hydrophobic pocket was almost fully occupied and bulkier groups appeared less likely to be accommodated. This presumption was consistent with the 20-fold activity difference in potency between compound 8 and compound 9, the former having a chlorine in the *para* position compared to the CF_3 group of the latter, which might begin to create a steric clash within the hydrophobic pocket. Finally, the trifluoromethoxy group on the 6-position of the pyrazolo-pyridine ring system is accommodated in a hydrophobic pocket, located at the entrance of the binding site. The pocket was created by three residues Val942, Leu905, Leu906 and Ile878 and hydrophobic interactions with these residues would contribute to the high potency of compound 22. Consistently, compound 14, which lacks a hydrophobic group at this position, showed much reduced potency. The strength of the hydrophobic interaction appears highly dependent on the size of the substituents. Compounds with substituents such as Cl (16) and CF_3 (15) showed moderate IC_{50} (< 1000 nM), while a decrease in potency was observed for compounds 23 and 24 which have bulkier aromatic substituents in this position.

Grandl and co-workers described mutations in the central region of S5 involved in the binding of an indazole compound that is structurally related to the compounds described here (*PLoS One*, September 2, 2014; DOI: 10.1371/journal.pone.0106776). These residues describe a region of the TRPA1 protein that is very close in space to the region shown in the figures above for the compounds in our study.

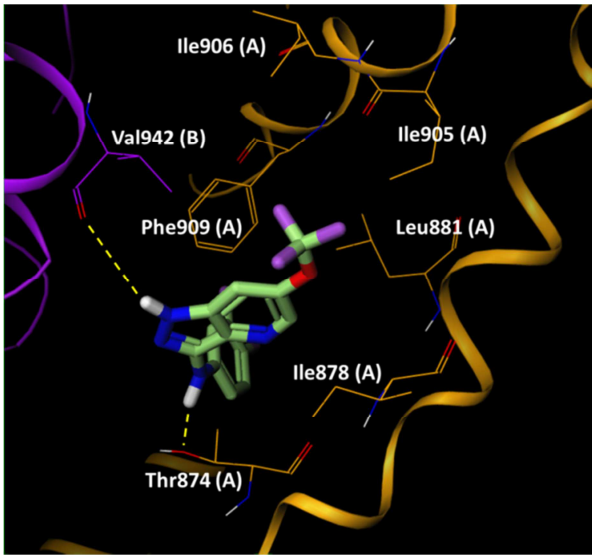

Supplementary Figure 3. Docked model of 22 in the cryo-EM structure of TRPA1. Only residues at the top of the binding site are highlighted for clarity. Residues from chain A and B are colored orange and purple respectively and highlighted residues are suffixed by chain ID for clarity.

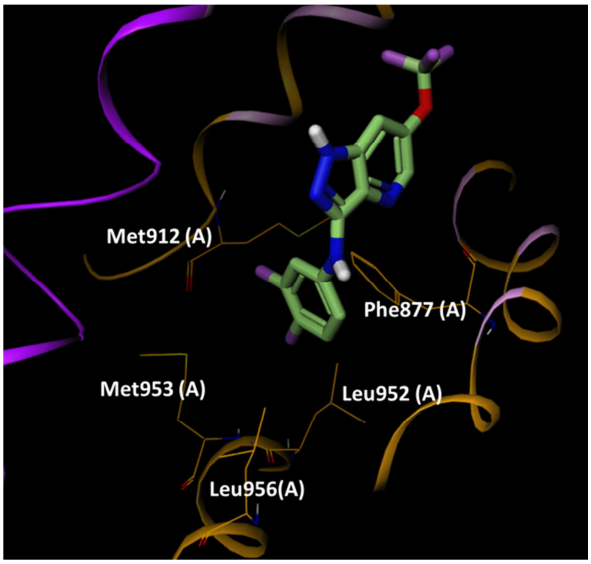

Supplementary Figure 4. Docked model of 22 in the cryo-EM structure of TRPA1. Only residues at the base of the binding site are highlighted for clarity. Residues from chain A and B are colored orange and purple respectively and highlighted residues are suffixed by chain ID for clarity.

7. AITC study

Adult Sprague-Dawley rats (Charles River Laboratories, Raleigh, NC) weighing 180-225g at time of testing were used in all experiments. Rats were housed four per cage and were maintained on a 12h light/dark cycle with lights on at 6 a.m. Rats had free access to food and water throughout the experiment and all experiments were conducted between 8 a.m. and 4 p.m. The experimental procedures described in this study adhered to the guidelines of the Committee for Research and Ethical Issues of the IASP, were approved by an Institutional Animal Care and Use Committee, and were performed in accordance with *The Guide for the Care and Use of Laboratory Animals*. Allyl isothiocyanate (AITC) was obtained from Sigma-Aldrich (St Louis, MO, USA) and the vehicle used was Neobe (Spectrum Chemicals, Northampton, UK). Morphine was obtained from Sigma-Aldrich (St Louis, MO, USA) and the vehicle used was 0.9% sterile saline. Methylcellulose was the vehicle used for all compounds. Separate experiments were conducted for each compound. Morphine (3.0 mg/kg, s.c.) was used as positive control for each experiment and was dosed 0.5 hr prior to behavioral evaluation. All test compounds and vehicles were dosed 2 hr prior to behavioural evaluation. One hour prior to behavioral evaluation rats were placed without restraint in a clear Plexiglass container to acclimate to the test environment. Immediately before testing, rats were restrained by hand and injected with 25µL of 10% AITC subcutaneously into the dorsal surface of the right hind paw. The rat was then placed without restraint into a Plexiglas observation chamber situated over an electromagnetic detector system (Automated Formalin Analyzer, Department of Anesthesiology, University of California, San Diego) and flinching behavior was recorded. Paw flinches of the AITC-injected paw are detected by the electromagnetic system and counted automatically using a computer. Measurements were be made for 30 minutes post AITC administration. All values are expressed as means ± standard error of the mean (SEM). All statistical analysis was carried out on the raw data using GraphPad Prism version 5.00 for Windows (GraphPad Software, San Diego California USA).

Compound 33 protein binding

Protein binding was measured using the equilibrium dialysis method, described in Riccardi, K.; Cawley, S.; Yates, P.D.; Chang, C.; Funk, C.; Niosi, M.; Lin, J and Di, L. *J. Pharm. Sci.* 2015, *104*(8), 2627-2636.

Human 98.2%

Rat 98.7%

Supplementary Table 3. Rat AITC efficacy and exposure data for 33

Comp	Minimum effective dose (mg/kg)	Free exposure (µM)	Rat MP potency (IC_{50})	Free exposure/ potency
33	100	0.166	0.195	0.9

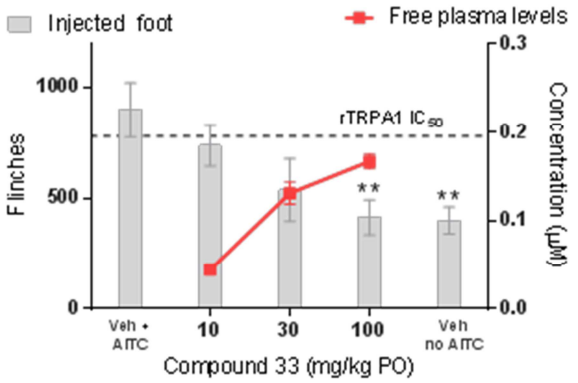

P<0.05 ANOVA with post hoc Dunnett's T-test

Supplementary Figure 5. Efficacy and PK/PD of 33 in a rat model of acute inflammatory pain

8. Laser Doppler sonography studies

All experimental procedures were conducted in accordance with UK Animals (Scientific Procedures) Act 1986 and followed the guidelines of the International Association for the Study of Pain (*Pain*, **1983**, *16*(2), 109-110). All studies were approved by the internal Pfizer governance committee for in vivo experiments.

Protein binding

Protein binding was measured using the equilibrium dialysis method, described in Riccardi, K.; Cawley, S.; Yates, P.D.; Chang, C.; Funk, C.; Niosi, M.; Lin, J and Di, L. *J. Pharm. Sci.* 2015, *104*(8), 2627-2636.

33

Human 98.2%

Rat 98.7%

22

Human 99.7%

Rat 99.2%

Compound 33 systemic study

Treatment groups

Male Sprague Dawley rats were weighed and randomised to one of the following treatment groups:

Group I: Vehicle (2ml/kg, PO)

Group II: 33 (10mg/kg, PO)

Group III: 33 (30mg/kg, PO)

Group IV: 33 (100mg/kg, PO)

Group V: 37 (300 mg/kg, PO), TRPV1 antagonist, negative control

The above mentioned treatment groups were dosed 180 min prior to cinnamaldehyde application.

Formulation and Dosing

33 was formulated in a homogenous suspension in 0.5% w/v methylcellulose/0.1% w/v Tween 80. 37 was formulated at 300 mg/kg in a homogenous suspension in 0.5% w/v methylcellulose/0.1% w/v Tween 80. 37 was supplied as a spray dried suspension form that contained 15% active pharmaceutical ingredient (API). *trans*-Cinnamaldehyde (99%, Sigma-Aldrich, Munich, Germany) was dissolved in 100% ethanol at 10% and 20% v/v and dosed topically at 50µl dose volume.

Laser Doppler imaging protocol

Male Sprague dawley rats were weighed and randomised to one of five treatment groups, orally dosed via gavage and returned to home cage. In all cases the experimenter was blinded to treatment group. 75 minutes following oral dosing, rats were placed in an anaesthetic chamber and anaesthetized with a 5% isoflurane/0_2 mix. Animals were then moved to a homoeothermic heat mat and anaesthesia maintained at approximately 2% isoflurane/O_2 during the laser Doppler scanning *via* nose cone for the duration of the study. The abdomen was then shaved to allow Laser Doppler flowmetry scans to be taken over an approximate area of 5 x 5 cm. This scan area was split into two equal halves to allow two doses of cinnamaldehyde to be applied. Baseline blood flow was measured for 35 minutes then 50µl of a 10% and 20% *trans*-cinnamaldehyde (99%, Sigma-Aldrich, Munich, Germany) dissolved in 100% ethanol was administered topically to the two halves of the scan area using a 12mm polypropylene coated aluminium Finn chamber on Scanpor tape (Biodiagnostics Ltd, Worcestershire) applied for a 10 minute duration. The Finn chamber was removed and Laser Doppler flowmetry scans were then recorded for 30 minutes.

Sample collection schedule

Terminal PK samples were taken from all animals via cardiac puncture at study endpoint (180 min post oral dose). Blood samples were centrifuged and resultant plasma samples were frozen at -20^{o}C prior to bioanalysis.

Supplementary Table 4.

	33						**37**	
Dose	**10mg/kg**		**30mg/kg**		**100mg/kg**		**300mg/kg**	
Conc^{n}	ng/mL	nM free	ng/mL	nM free	ng/mL	nM free	ng/mL	nM free
Mean	28	12	114	48	127	53	355	1087

	4				4		5	
SD	85	4	430	18	491	21	1250	382

Equipment and supplies list

MoorLDI2 laser Doppler imager (Moor Instruments Ltd, Axminster, UK).

Data analysis

All data design, randomization and analysis were handled in accordance with previous discussions with Non-Clinical Statistics group. In brief, area under the curve (AUC) analysis was carried out for normalized blood flow following cinnamaldehyde challenge. AUC values were then compared across groups using one-way ANOVA.

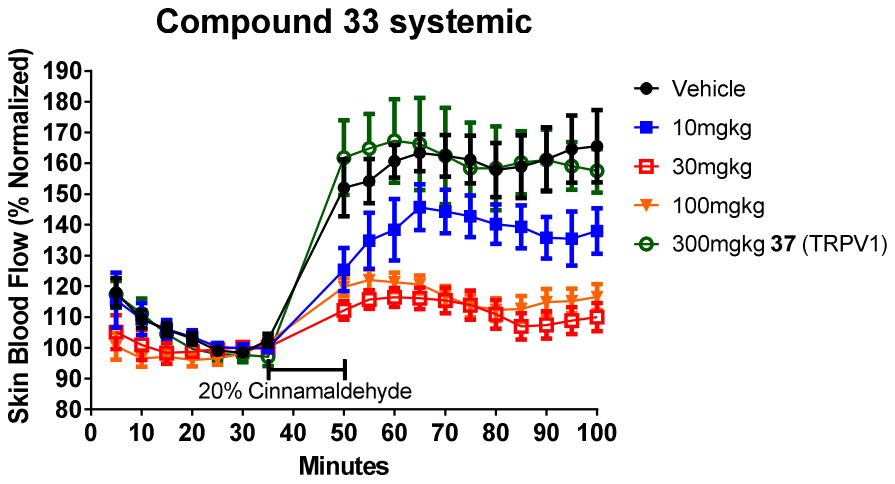

Supplementary Figure 6. Cinnamaldehyde flare response data with systemically applied 33

Compound 22 topical study

Treatment groups

Male Sprague dawley rats were weighed and randomised to one of the following treatment groups:

Group I: Vehicle (5µl/cm^2, Topical); 30 minute pre-dose.

Group II: 22, 50mg/ml (5µl/cm^2, Topical); 30 minute pre-dose.

Group III: Vehicle (5µl/cm^2, Topical); 60 minute pre-dose.

Group IV: 22, 50mg/ml (5µl/cm^2, Topical); 60 minute pre-dose.

Formulation and dosing

22 was formulated into a solution of 70:30 ethanol: propylene glycol and dosed at 6 µl/cm^2. To a weighing of the compound (equivalent to a final concentration of 50 mg/mL), ethanol was added to 70% of the final volume. This was sonicated until dissolved, prior to addition of 30% of final volume of propylene glycol. This was mixed well to give a final clear solution for dosing. *trans*-Cinnamaldehyde (99%, Sigma-Aldrich, Munich, Germany) was dissolved in 100% ethanol at 20% v/v and dosed topically at 50µl dose volume.

Laser Doppler imaging protocol

Male Sprague Dawley rats were weighed and randomised to one of the 4 treatment groups, placed in an anaesthetic chamber and anaesthetized with a 5% isoflurane/0_2 mix. Animals were then moved to a homoeothermic heat mat and anaesthesia maintained at approximately 2% isoflurane/O_2 during the laser Doppler scanning via nose cone for the duration of the study.

The abdomen was then shaved to allow Laser Doppler flowmetry scans to be taken over an approximate area of 2.5 cm^2. Baseline scans were recorded for 10mins, subsequently 15µl of compound (50mg/ml 22) or vehicle (70:30 ethanol: propylene glycol) was then applied to the centre of the scan area. The treatment was left to penetrate the skin for 30 or 60 minutes while baseline blood flow was measured. After the treatment period, a further 5 post-dose Doppler scans were completed to establish a post-dose baseline before 50µl of 20% *trans*-cinnamaldehyde (99%, Sigma-Aldrich, Munich, Germany) dissolved in 100% ethanol was administered topically to the centre of the scan area using a 12mm polypropylene coated aluminium Finn chamber on Scanpor tape (Biodiagnostics Ltd, Worcestershire) applied for a 10 minute period. The Finn chamber was removed and Laser Doppler flowmetry scans were then recorded for 30 minutes.

Sample collection schedule

Terminal PK samples were taken from all animals via cardiac puncture at study endpoint (70-120 min post topical dose depending on pre-dose time). Blood samples were centrifuged and resultant plasma samples were frozen at -20^{o}C prior to bioanalysis.

Supplementary Table 5.

Animal	1	2	3	4	5	6	7	8
	22							
Dose	**50 mg/mL**							
Total ng/mL	1936	512	1512	1361	454	221	702	709
nM free	59	16	46	41	14	7	21	22

Equipment and supplies list

MoorLDI2 laser Doppler imager (Moor Instruments Ltd, Axminster, UK).

Data analysis

All data design, randomization and analysis were handled in accordance with previous discussions with Non-Clinical Stats group. In brief, area under the curve (AUC) analysis was carried out for normalized blood flow following cinnamaldehyde challenge. AUC values were then compared across groups using one-way ANOVA.

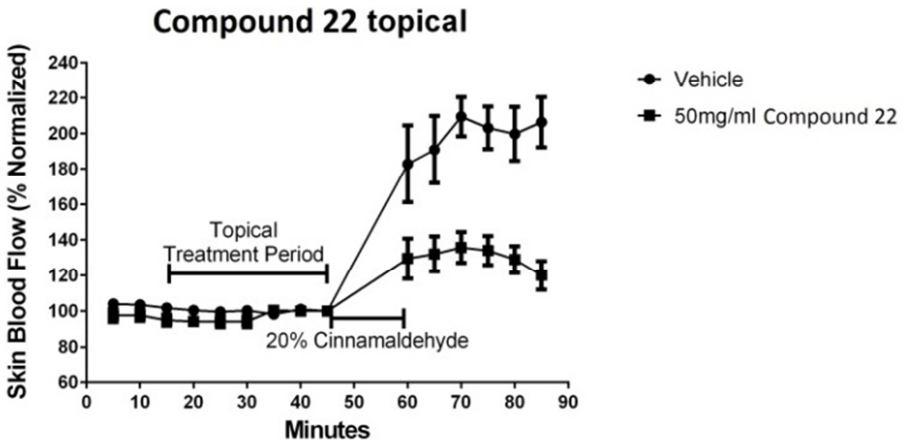

Supplementary Figure 7. Cinnamaldehyde flare response data with topically applied 22 and a 30min pre-incubation period

9. Supplementary references

TRPA1 as a drug discovery target

(a) Chen, J.; McGaraughty, S. and Kym, P.R. *TRPA1 in Drug Discovery.* In *TRP Channels in Drug Discovery*. Vol. 1; Szallasi, A. and Biro, T. Eds; Springer: 2012; pp43-60.

(b) Chen, J. and Hackos, D.H. TRPA1 as a Drug Target – Promise and Challenges. *Arch. Pharmacol*., 2015, *388*(4), 451-463.

TRPA1 acts as a chemosensor for electrophilic ligands

(a) Jordt, S.E.; Bautista, D.M.; Chuang, H.H.; McKemy, D.D.; Zygmunt, P.M.; Hogestatt, E.D.; Meng, I.D. and Julius, D. Mustard Oils and Cannabinoids Excite Sensory Nerve Fibres Through the TRP channel ANKTM1. *Nature* **2004**, *427*(6971), 260-265.

(b) Talavera, K.; Gees, M.; Karashima, Y.; Meseguer, V.M.; Vanoirbeek, J.A.; Damann, N.; Everaerts, W.; Wouter, B.; Benoit, M.; Janssens, A.; Vennekens, R.; Viana, F.; Benoit, N.; Nilius, B. and Voets, T. Nicotine Activates the Chemosensory Cation Channel TRPA1. *Nat*. *Neurosci*. **2009**, *12*, 1293-1299.

The TRPA1 channel is linked to pain sensation and hyperalgesia

(a) Nassini, R.; Materazzi, S.; Benemei, S. and Geppetti, P. The TRPA1 Channel in Inflammatory and Neuropathic Pain and Migraine. In *Reviews of Physiology Biochemistry and Pharmacology*. Vol 167; Nilius, B.; Gudermann, T.; Jahn, R.; Lill, R.; Offermanns, S. and Petersen, O.H. Eds., Springer: 2014, pp1-43.

(b) Kaneko, Y. and Szallasi, A. Transient Receptor Potential (TRP) Channels: a Clinical Perspective. *Br. J. Pharmacol.*, **2014**, *171*(10), 2474-2507.

(c) Brederson, J.-D.; Kym, P.R. and Szallasi, A. Targeting TRP Channels for Pain Relief. *Eu. J. Pharmacol.*, **2013**, *716*(1-3), 61-76.

TRPA1 antagonism may reverse pain in rodent models

(a) McGaraughty, S.; Chu, K.L.; Perner, R.J.; DiDomenico, S.; Kort, M.E. and Kym, P.R. TRPA1 Modulation of Spontaneous and Mechanically Evoked Firing of Spinal Neurons in Uninjured, Osteoarthritic, and Inflamed Rats. *Mol. Pain*, March 5, 2010; DOI: 10.1186/1744-8069-6-14.

(b) Chen, J.; Joshi, S.K.; DiDomenico, S.; Perner, R.J.; Mikusa, J.P.; Gauvin, D.M.; Segreti, J.A.; Han, P.; Zhang, X-F.; Niforatos, W.; Bianchi, B.R.; Baker, S.J.; Zhong, C.; Simler, G.H.; McDonald, H.A.;

Schmidt, R.G.; McGaraughty, S.P.; Chu, K.L.; Faltynek, C.L.; Kort, M.E.; Reilly R.M. and Kym, P.R. Selective Blockade of TRPA1 Channel Attenuates Pathogical Pain Without Altering Noxious Cold Sensation or Body Temperature. *Pain*, **2011**, *152*(5), 1165-1172.

(c) da Costa, D.S.; Meotti, F.C.; Andrade, E.L.; Leal, P.C.; Motta, E.M. and Calixto, J.B. The Involvement of the Transient Receptor Potential A1 (TRPA1) in the Maintenance of Mechanical and Cold Hyperalgesia in Persistent Inflammation. *Pain*, **2010**, *148*(3), 431-437.

Reported TRPA1 antagonist series in the patent and journal literature

(a) Baraldi, P.G.; Romagnoli, R.; Saponaro, G.; Tabrizi, M.A.; Baraldi, S.; Pedretti, P.; Fusi, C.; Nassini, R.; Materazzi, S.; Geppetti, P. and Preti, D. 7-Substituted-pyrrolo[3,2-d]pyrimidine-2,4-dione Derivatives as Antagonists of the Transient Receptor Potential Ankyrin 1 (TRPA1) Channel: a Promising Approach for Treating Pain and Inflammation. *Bioorg. Med. Chem*. 2012, *20*(5), 1690-1698.

(b) Vallin, K.S.A.; Sterky, K.J.; Nyman, E.; Bernstrom, J.; From, R.; Linde, C.; Minidis, A.B.E.; Nolting, A.; Narhi, K.; Santangelo, E.M.; Sehgelmeble, F.W.; Sohn, D.; Strindlund J. and Weigelt, D. N-1-Alkyl-2-oxo-2-aryl Amides as Novel Antagonists of the TRPA1 Receptor. *Bioorg. Med. Chem*. 2012, *22*(17), 5485-5492.

(c) Ortar, G.; Moriello, A.S.; Morera, E.; Nalli, M.; Di Marzo, V. and De Petrocellis, L. 3-Ylidenephthalides as a New Class of Transient Receptor Potential Channel TRPA1 and TRPM8 Modulators. *Bioorg. Med. Chem. Lett*. 2013, *23*(20), 5614-5618;

(d) Morera, E.; De Petrocellis, L.; Morera, L.; Moriello, A.S.; Nalli, M.; Di Marzo, V. and Ortar, G. Synthesis and Biological Evaluation of [6]-gingerol Analogues as Transient Receptor Potential Channel TRPV1 and TRPA1 Modulators. *Bioorg. Med. Chem. Lett*. 2012, *22*(4), 1674-1677.

(e) Baraldi, P.G.; Preti, D.; Materazzi, S. and Geppetti, P. Transient Receptor Potantial Ankyrin 1 (TRPA1) Channel as Emerging Target for Novel Anagesics and Anti-Inflammatory Agents. *J. Med. Chem*. 2010, *53*(14), 5085-5107.

(f) Salat, K.; Moniczewski, A. and Librowski, T. Transient Receptor Potential Channels – Emerging Novel Drug Targets for the Treatment of Pain. *Curr. Med. Chem*. 2013, *20*(11), 1409-1436.

(g) Waskielewicz, A.M.; Gunia, A.; Szkaradek, N.; Sloczynska, K.; Krupinska, S. and Marona, H. Ion Channels as Drug Targets in Central Nervous System Disorders. *Curr. Med. Chem*. 2013, *20*(10), 1241-1285.

(h) Rooney, L.; Vidal, A.; D-Souza, A-M.; Devereux, N.; Masick, B.; Boissel, V.; West, R.; Head, V.; Stringer, R.; Lao, J.; Petrus, M.J.; Patapoutian, A.; Nash, M.; Stoakley, N.; Panesar, M.; Verkuyl, J.M.; Schumacher, A.M.; Petrassi H.M. and Tully, D.C. Discovery, Optimization, and Biological Evaluation of 5-(2-(Trifluoromethyl)phenyl)indazoles as a Novel Class of Transient Receptor Potential A1 (TRPA1) Antagonists. *J. Med. Chem*., 2014, *57*(12), 5129-5140.

(i) Hu, Y-J.; St-Onge, M.; Laliberté, S.; Vallee, F.; Jin, S.; Bedard, L.; Labrecque J. and Albert, J.S. Discovery of a 4-Aryloxy-1H-pyrrolo[3,2-c]pyridine and a 1-Aryloxyisoquinoline Series of TRPA1 Antagonists. *Bioorg. Med. Chem. Letts*., 2014, *24*(14), 3199-3203.

(j) Laliberté, S.; Vallee, F.; Fournier, P-A.; Bedard, L.; Labrecque J. and Albert, J.S. Discovery of a Series of Aryl-N-(3-(alkylamino)-5-(trifluoromethyl)phenyl)benzamides as TRPA1 Antagonists. *Bioorg. Med. Chem. Letts*., 2014, *24*(14), 3204-3206.

(k) Copeland, K.W.; Boezio, A.A.; Cheung, E.; Lee, J.; Olivieri, P.; Schenkel, L.B.; Wan, Q.; Wang, W.; Wells, M.C.; Youngblood, B.; Gawa, N.R.; Lehto, S.G. and Geuns-Meyer, S. Development of Novel Azabenzofuran TRPA1 antagonists as in Vivo Tools, *Bioorg. Med. Chem. Letts*., 2014, *24*(15), 3464-3468.

(l) Schenkel, L.B.; Olivieri, P.; Boezio, A.A.; Deak, H.L.; Emkey, R.; Graceffa, R.F.; Gunaydin, H.; Guzman-Perez, A.; Lee, J.H.; Teffera, Y.; Wang, W.; Youngblood, B.D.; Yu, V.L.; Zhang, M.; Gavva, N.R.; Lehto, S.G. and Geuns-Meyer, S. Optimization of a Novel Quinazoline-Based Series of Transient Receptor Potential A1 (TRPA1) Antagonists Demonstrating Potent in Vivo Activity, *J. Med. Chem*., 2016, 69(6), 2794-2809.

Recent TRPA1 structure-function studies

(a) Xiao, B.; Dubin, A.E.; Bursulaya, B.; Viswanath, V.; Jegla, T.J. and Patapoutian, A. Identification of Transmembrane Domain 5 as a Critical Molecular Determinant of Menthol Sensitivity in Mammalian TRPA1 Channels. *J Neurosci*, 2008, *28*(39), 9640-9651.

(b) Nakatsuka, K.; Gupta, R.; Saito, S.; Banzawa, N.; Takahashi, K.; Tominaga, M. and Ohta, T. Identification of Molecular Determinants for a Potent Mammalian TRPA1 Antagonist by Utilizing Species Differences. *J Mol Neurosci*, 2013, *51*(3), 754-762.

(c) Paulsen, C.E.; Armache, J-P.; Gao, Y.; Cheng, Y. and Julius, D. Structure of the TRPA1 Ion Channel Suggests Regulatory Mechanisms. *Nature*, 2015, *520*, 511-517.

Recent paper from this group on an alternative TRPA1 series, and a description of using protein chimeras to elucidate binding region

Pryde, D. C.; Marron, B.; West, C.G.; Reister, S.; Amato, G.; Yoger, K.; Padilla, K.; Turner, J.; Swain, N. A.; Cox, P. J.; Skerratt, S.E.; Ryckmans, T.; Blakemore, D.C.; Warmus, J. and Gerlach A. C., The Discovery of a Potent Series of Carboxamide TRPA1 Antagonists, *MedChemComm*, 2016, *7*, 2145-2158.

All studies were conducted according to the guidelines issued by the International Association for the Study of Pain, and all protocols were reviewed and approved by an internal governance committee

Zimmerman, M. Ethical Guidelines for Investigations of Experimental Pain in Conscious Animals. *Pain*, 1983, *16*(2), 109-110.

References describing the metabolism assays used

(a) Allan, G.; Davis, J.; Dickins, M.; Gardner, I.; Jenkins, T.; Jones, H.; Webster, R.; Westgate, H. Pre-clinical Pharmacokinetics of UK-453,061, a Novel Non-nucleoside Reverse Transcriptase Inhibitor (NNRTI), and Use of in silico Physiologically-based Prediction Tools to Predict the Oral Phramcokinetics of UK-453,061 in Man. *Xenobiotica*, **2008**, *38*, 620-640.

(b) Feng, B.; Mills, J.B.; Davidson, R.E.; Mireles, R.J.; Janiszewski, J.S.; Troutman, M.D. and de Morais, S.M. In vitro P-glycoprotein Assays to Predict the in vivo Interactions of P-glycoprotein with Drugs in the Central Nervous System. *Drug Met. Disp.*, **2008**, *36*, 268-275.

(c) Di, L.; Whitney-Pickett, C.; Umland, J.P.; Zhang, H.; Zhang, X.; Gebhard, D.F.; Lai, Y.; Federico, J.J.; Davidson, R.E.; Smith, R.; Reyner, E.L.; Lee, C.; Feng, B.; Rotter, C.; Varma, M.V.; Kempshall, S.; Fenner, K.; El-Kattan, A.F.; Liston, T.E.; Troutman, M.D. Development of a New Permeability Assay Using Low-efflux MDCKII Cells. *J. Pharm. Sci*. **2011**, *100*(11), 4974-4985.

10. Selected NMR spectra

Compound 17

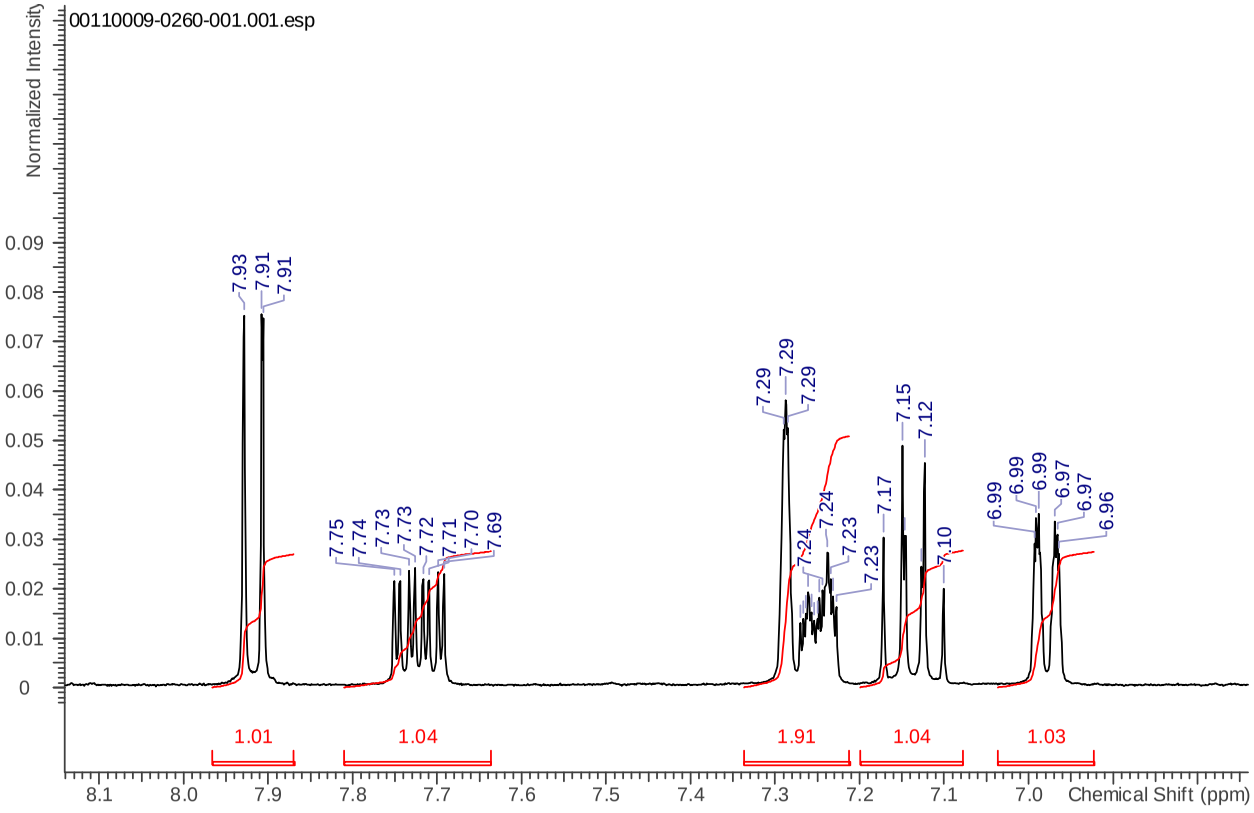
00110009-0260-001.001.esp
Normalized Intensity
0.09
0.08
0.07
0.06
0.05
0.04
0.03
0.02
0.01
0
7.93
7.91
7.91
7.75
7.74
7.73
7.73
7.72
7.71
7.70
7.69
7.29
7.29
7.29
7.24
7.24
7.23
7.23
7.17
7.15
7.12
7.10
6.99
6.99
6.99
6.97
6.97
6.96
1.01
1.04
1.91
1.04
1.03
8.1
8.0
7.9
7.8
7.7
7.6
7.5
7.4
7.3
7.2
7.1
7.0
Chemical Shift (ppm)

Compound 18

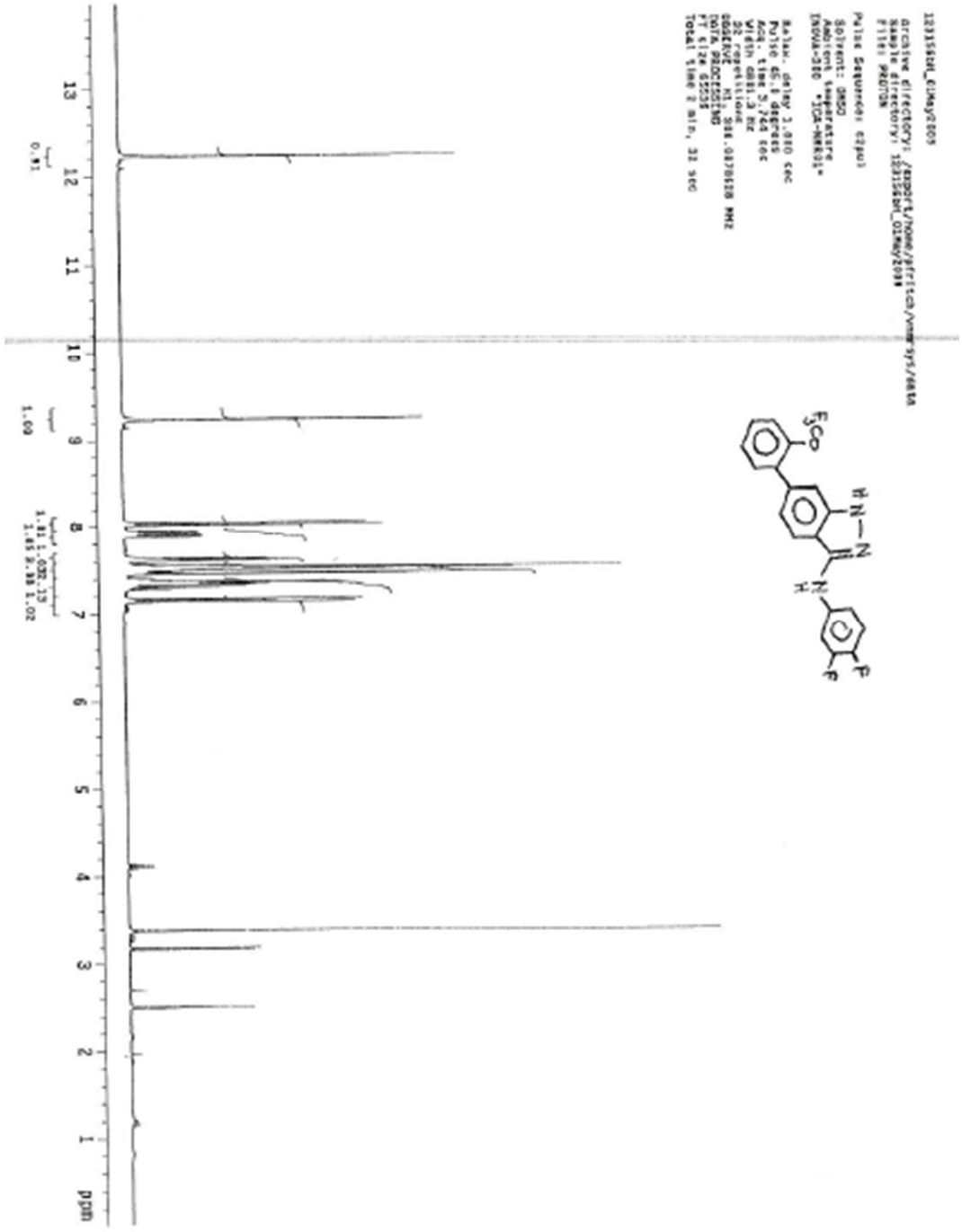

Compound 20

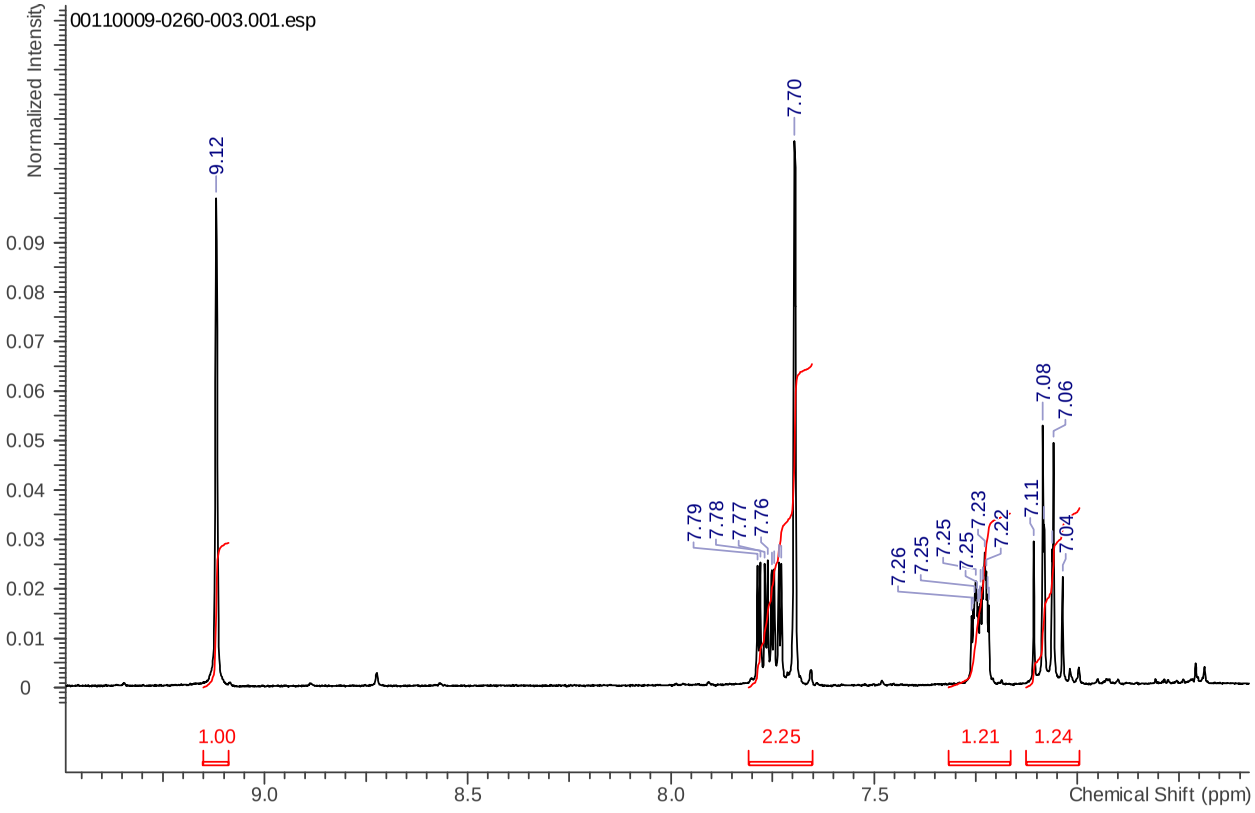
00110009-0260-003.001.esp
Normalized Intensity
9.12
7.70
7.79
7.78
7.77
7.76
7.26
7.25
7.25
7.23
7.22
7.11
7.08
7.06
7.04
1.00
2.25
1.21
1.24
Chemical Shift (ppm)

Compound 22

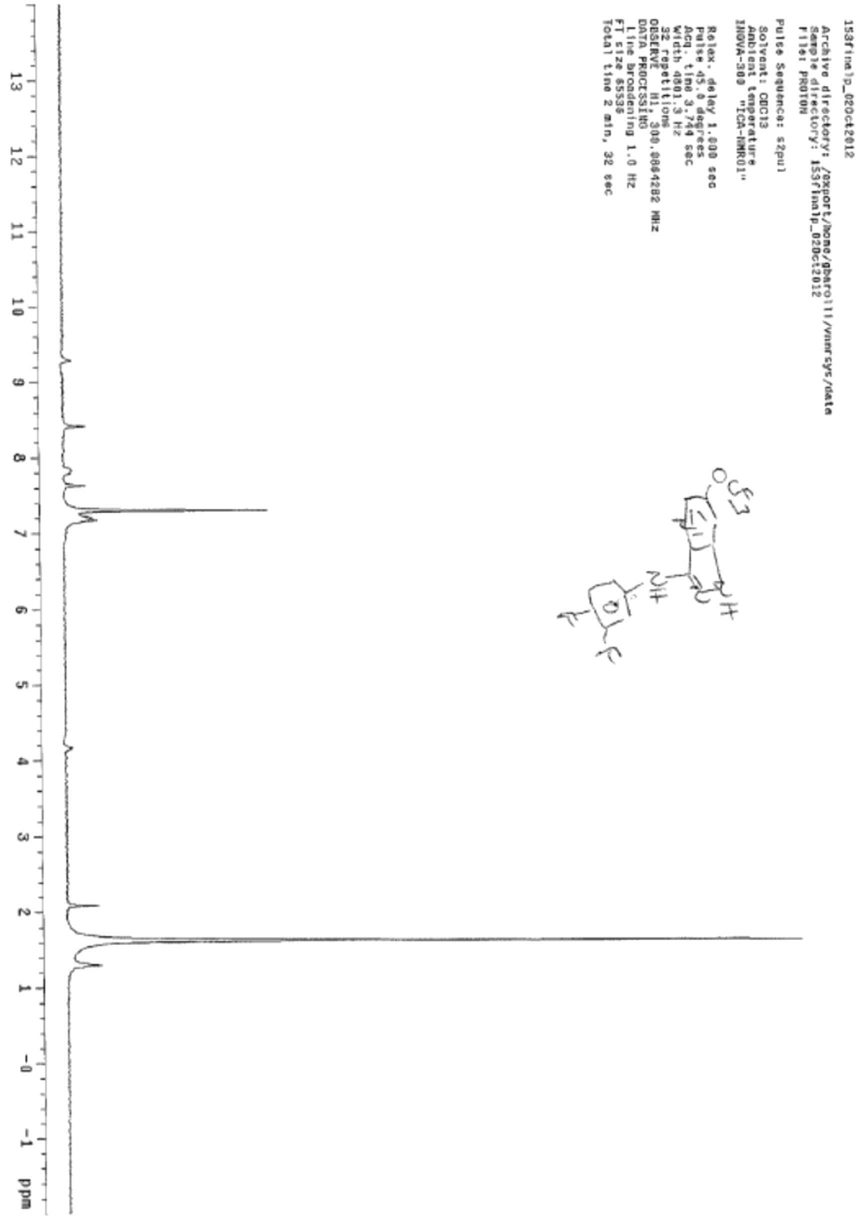
153finalp_02Oct2012
Archive directory: /export/home/gbaroilli/vnmrsys/data
Sample directory: 153finalp_02Oct2012
File: PROTON
Pulse Sequence: s2pul
Solvent: CDCl3
Ambient temperature
INOVA-300 "ICA-NMR01"
Relax. delay 1.000 sec
Pulse 45.0 degrees
Acq. time 3.744 sec
Width 4801.3 Hz
32 repetitions
OBSERVE H1, 300.0864282 MHz
DATA PROCESSING
Line broadening 1.0 Hz
FT size 65536
Total time 2 min, 32 sec
13
12
11
10
9
8
7
6
5
4
3
2
1
-0
-1
ppm

Compound 28

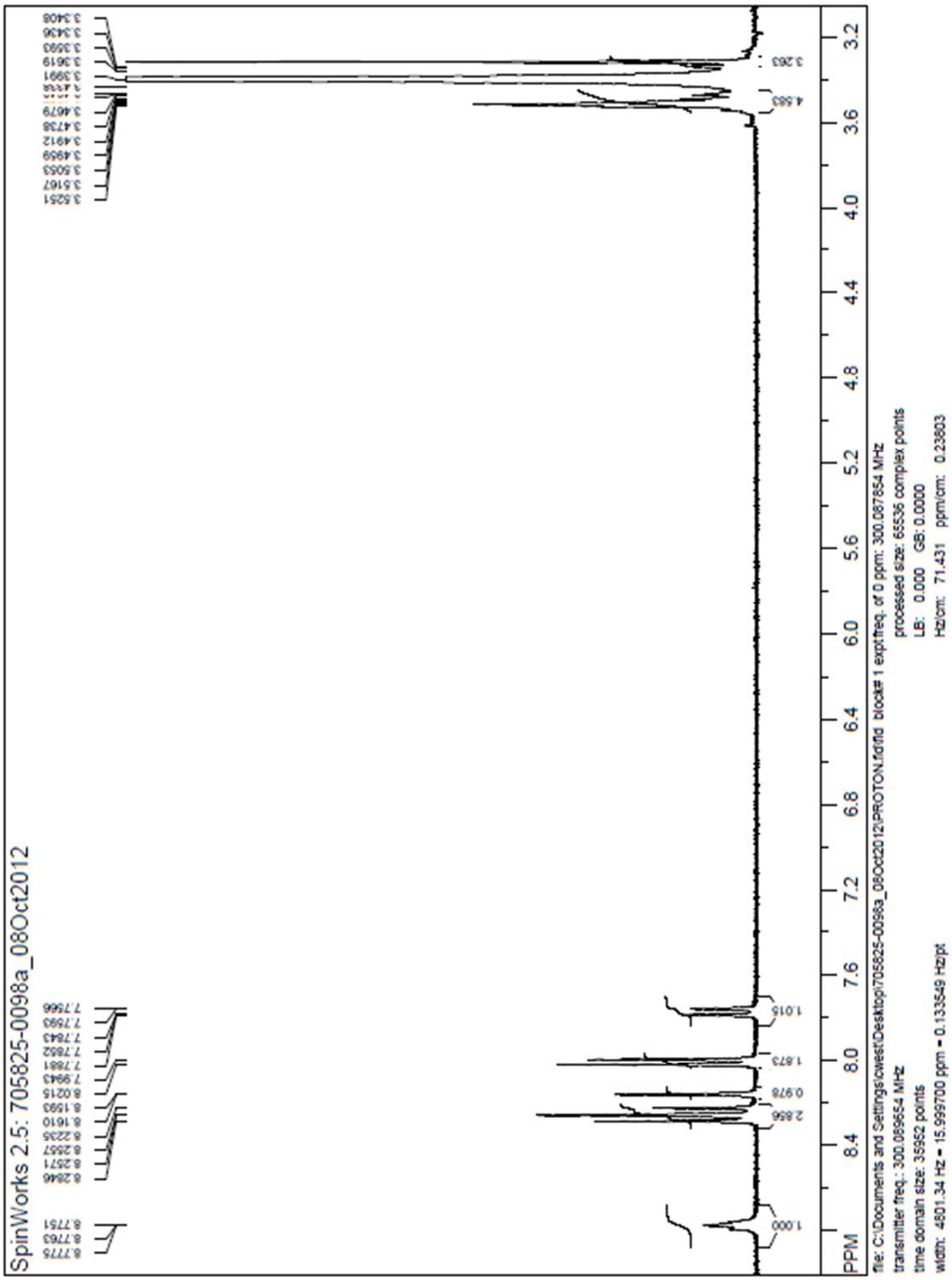
SpinWorks 2.5: 705825-0098a_08Oct2012
8.7775
8.7763
8.7751
8.2846
8.2571
8.2357
8.2236
8.1610
8.1593
8.0215
7.9943
7.7881
7.7852
7.7843
7.7830
7.7566
3.5251
3.5167
3.5053
3.4959
3.4912
3.4738
3.4679
3.3991
3.3619
3.3593
3.3436
3.3408
1.000
2.866
0.978
1.873
1.015
4.883
3.263
PPM
8.4
8.0
7.6
7.2
6.8
6.4
6.0
5.6
5.2
4.8
4.4
4.0
3.6
3.2
file: C:\Documents and Settings\cswest\Desktop\705825-0098a_08Oct2012\PROTON.fid/fid block# 1 exptfreq. of 0 ppm: 300.087854 MHz
transmitter freq.: 300.089654 MHz
time domain size: 35952 points
width: 4801.34 Hz = 15.999700 ppm = 0.133549 Hz/pt
number of scans: 32
processed size: 65536 complex points
LB: 0.000 GB: 0.0000
Hz/cm: 71.431 ppm/cm: 0.23803

Compound 31

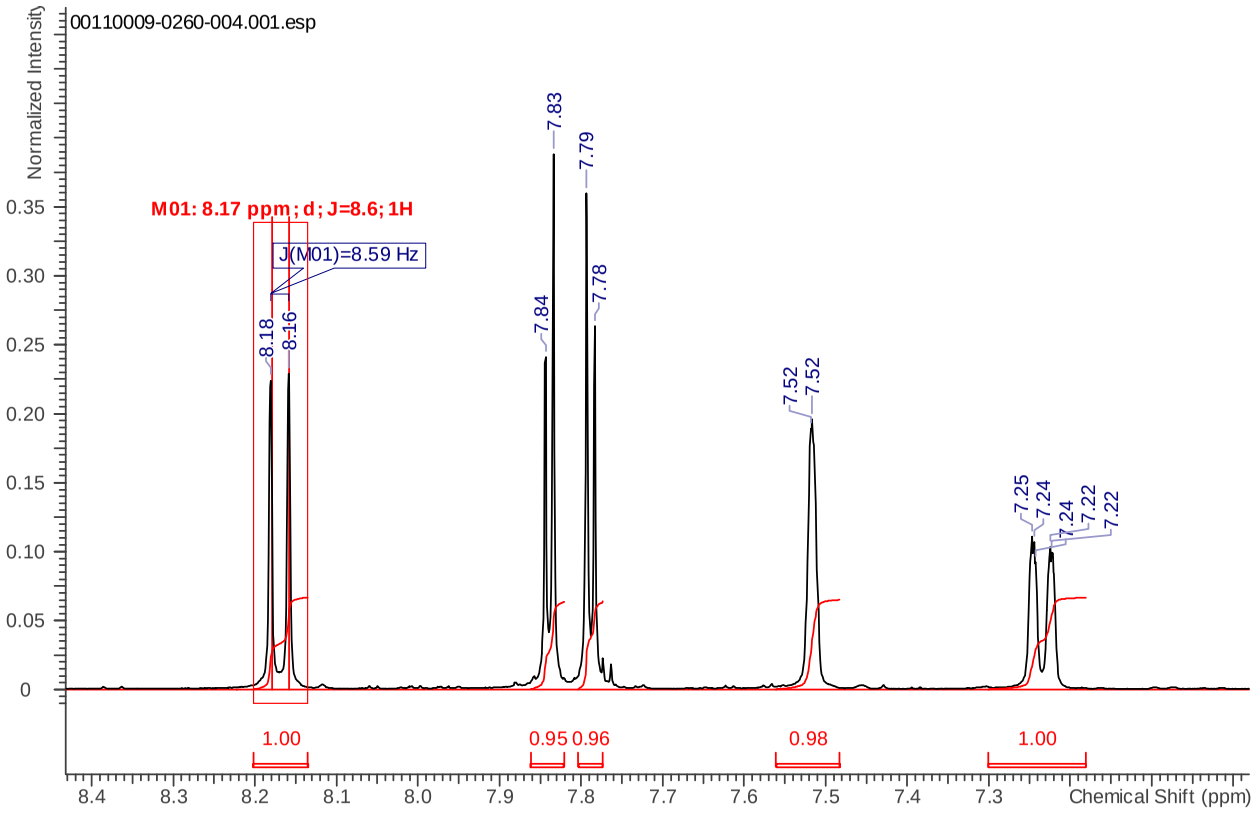
00110009-0260-004.001.esp
Normalized Intensity
M01: 8.17 ppm ; d ; J=8.6; 1H
J(M01)=8.59 Hz
8.18
8.16
7.84
7.83
7.79
7.78
7.52
7.52
7.25
7.24
7.24
7.22
7.22
1.00
0.95
0.96
0.98
1.00
Chemical Shift (ppm)

Compound 32

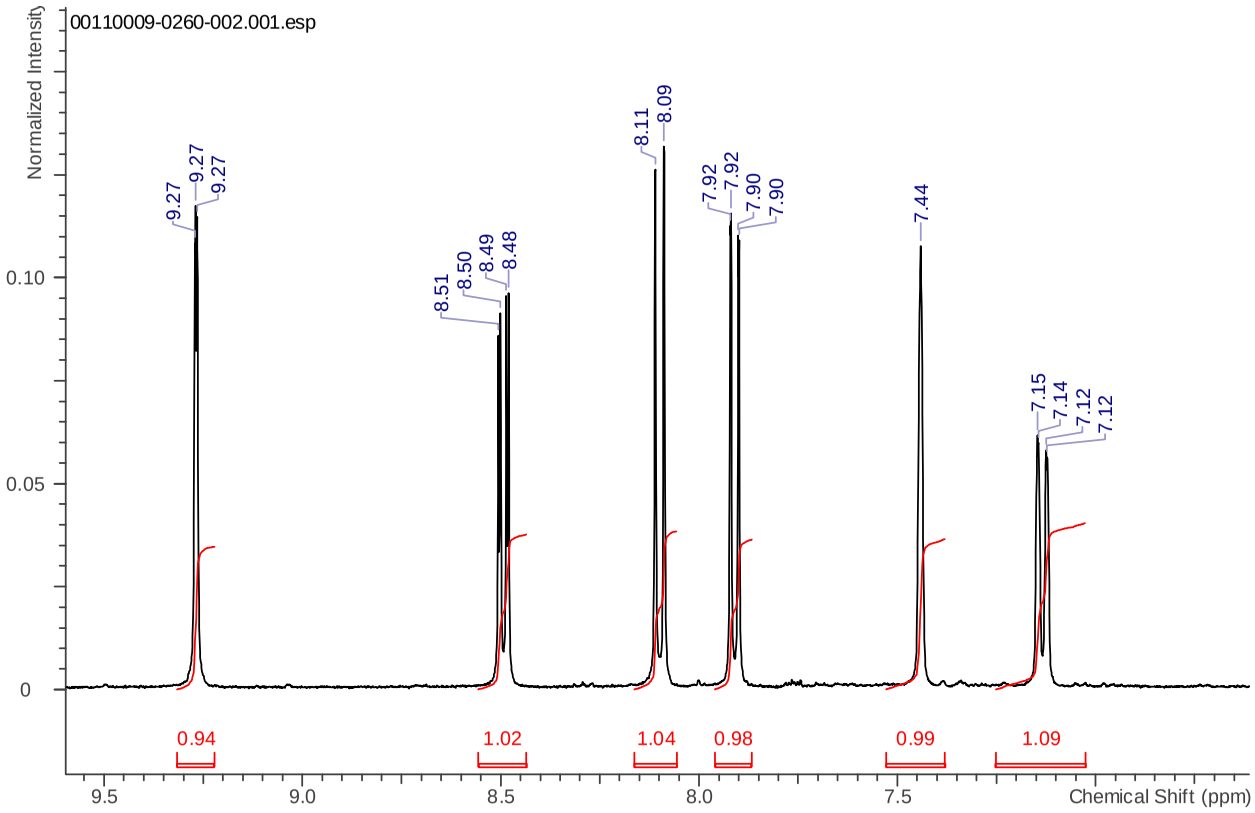
00110009-0260-002.001.esp
Normalized Intensity
0.10
0.05
0
9.27
9.27
9.27
8.51
8.50
8.49
8.48
8.11
8.09
7.92
7.92
7.90
7.90
7.44
7.15
7.14
7.12
7.12
0.94
1.02
1.04
0.98
0.99
1.09
9.5
9.0
8.5
8.0
7.5
Chemical Shift (ppm)

Compound 33

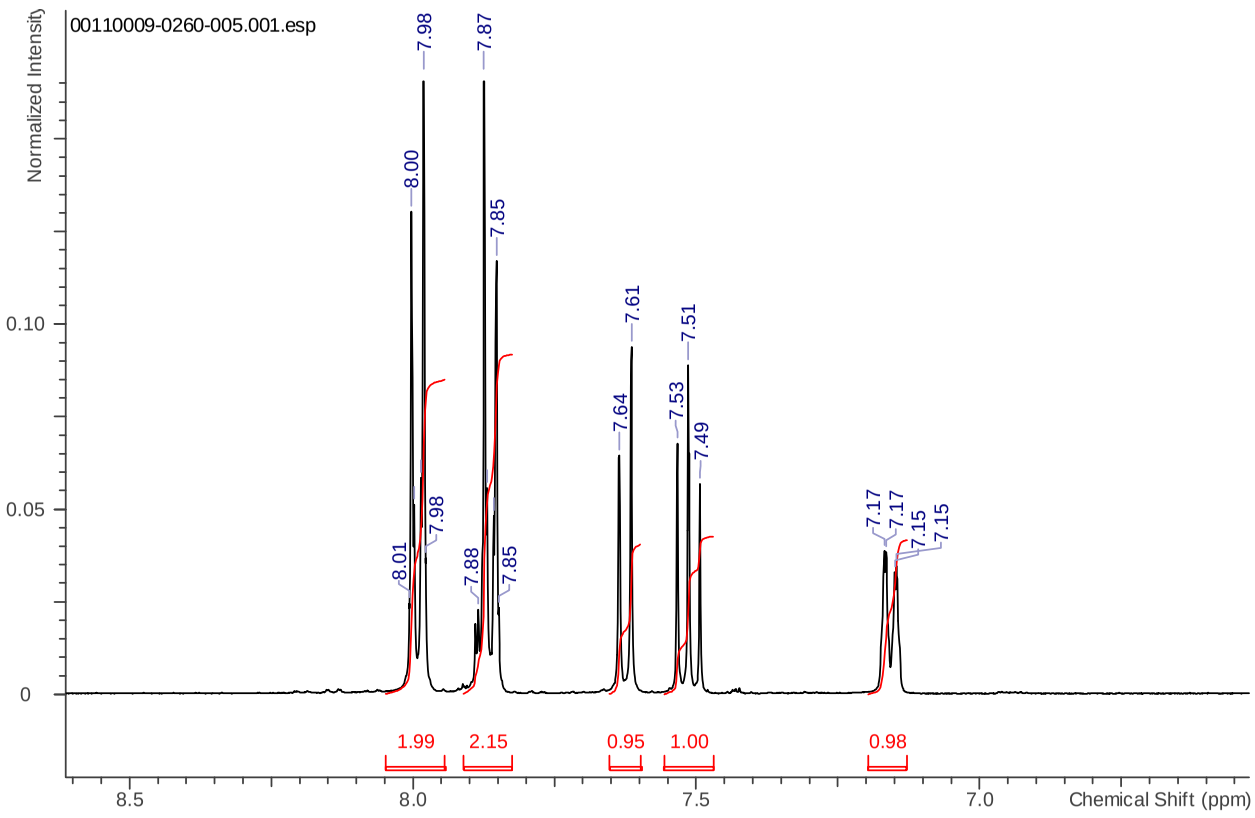
00110009-0260-005.001.esp
Normalized Intensity
0.10
0.05
0
8.01
7.98
8.00
7.98
7.88
7.87
7.85
7.85
7.64
7.61
7.53
7.51
7.49
7.17
7.17
7.15
7.15
1.99
2.15
0.95
1.00
0.98
8.5
8.0
7.5
7.0
Chemical Shift (ppm)

Compound 34